Spring 2011

A numerical method for solving the elliptic and elasticity interface problems

Liqun Wang

A NUMERICAL METHOD FOR SOLVING THE ELLIPTIC AND ELASTICITY INTERFACE PROBLEMS

by

Liqun Wang, B S , M S

A Dissertation Presented in Partial Fulfillment
of the Requirements for the Degree
Doctor of Philosophy

COLLEGE OF ENGINEERING AND SCIENCE
LOUISIANA TECH UNIVERSITY

May 2011

LOUISIANA TECH UNIVERSITY

THE GRADUATE SCHOOL

04/07/2011

Date

We hereby recommend that the dissertation prepared under our supervision by Liqun Wang

entitled

A Numerical Method for Solving the Elliptic and Elasticity Interface Problems

be accepted in partial fulfillment of the requirements for the Degree of

Ph D in Computational Analysis and Modeling

Supervisor of Dissertation Research

Head of Department

Computational Analysis and Modeling

Department

Recommendation concurred in

Advisory Committee

Approved

Director of Graduate Studies

Dean of the College

Approved

Dean of the Graduate School

GS Form 13a
(6/07)

ABSTRACT

Interface problems arise when dealing with physical problems composed of different materials or of the same material at different states. Because of the irregularity along interfaces, many common numerical methods do not work, or work poorly, for interface problems. Matrix-coefficient elliptic and elasticity equations with oscillatory solutions and sharp-edged interfaces are especially complicated and challenging for most existing methods. An accurate and efficient method is desired.

In 1999, the boundary condition capturing method was proposed to deal with Poisson equations with interfaces whose variable coefficients and solutions may be discontinuous. In 2003, a weak formulation was derived. Built on previous work that solves elliptic interface problems with two domains in two dimensions, this dissertation improves the accuracy in the presence of sharp-edged interfaces and extends to elasticity interface problems with two domains in two dimensions, elliptic interface problems with three domains in two dimensions, and elliptic interface problems with two domains in three dimensions.

The method used in this dissertation is a non-traditional finite element method. The test function basis is chosen to be the standard finite element basis independent of the interface, and the solution basis is chosen to be piecewise linear, satisfying the jump conditions across the interface. These two bases are different, which leads to the non-symmetric matrix generated by this method, but the resulting linear system

of equations is shown to be positive definite under certain assumptions in all the four topics mentioned in this dissertation This method has matrix coefficients and lower-order terms, and uses the non-body-fitting grid, which makes it easy to deal with different kinds of interfaces, like the examples “Star”, “Happy face”, “Chess board”, to name a few

The methods used in this dissertation solve the non-smooth interface case and promise results for oscillatory solutions Numerical experiments show that this method is second-order accurate in the L^{∞} norm for piecewise smooth solutions

APPROVAL FOR SCHOLARLY DISSEMINATION

The author grants to the Prescott Memorial Library of Louisiana Tech University the right to reproduce, by appropriate methods, upon request, any or all portions of this Dissertation It is understood that "proper request" consists of the agreement, on the part of the requesting party, that said reproduction is for his personal use and that subsequent reproduction will not occur without written approval of the author of this Dissertation Further, any portions of the Dissertation used in books, papers, and other works must be appropriately referenced to this Dissertation

Finally, the author of this Dissertation reserves the right to publish freely, in the literature, at any time, any or all portions of this Dissertation

Author

Date 05/03/2011

GS Form 14
(5/03)

TABLE OF CONTENTS

LIST OF TABLES

LIST OF FIGURES

NOMENCLATURE

Ω	Whole domain
$\overline{\Omega}$	Closure of the domain
$\Omega^{\pm}$	Subdomain
$\partial\Omega$	Boundary of the domain
Γ	Interface
(u, v) or $u \quad v$	$u \quad v = \sum_{i=1}^{n}(u_i v_i)$
∇u	$\nabla u = (\partial_1 u, \partial_2 u, \qquad, \partial_n u)^T$
$\nabla \quad u$	$\nabla \quad u = \sum_{i=1}^{n}(\partial_i u_i)$
$L^2(\Omega)$	$\{u \quad u$ is defined on Ω, and $\int_{\Omega} u^2 dx < \infty\}$
$H^1(\Omega)$	$\{u \quad u$ and ∇u belong to $L^2(\Omega)\}$
$H_0^1(\Omega)$	$\{u \in H^1(\Omega) \quad u = 0$ on $\partial\Omega\}$
L^∞ norm	$\lVert x \rVert_\infty = max\{\lvert x_1\rvert, \lvert x_2\rvert, \qquad, \lvert x_n\rvert\}$
χ_Ω	$\chi_\Omega = \begin{cases} 1 & \text{in } \Omega \\ 0 & \text{otherwise} \end{cases}$
Γ_K^h	Interface segment in two dimensions
Γ_L^h	Interface segment in three dimensions
$\triangle_k$	Interface cell in two dimensions

$\blacktriangle_k$	Interface cell in three dimensions
ϕ	level-set function
n	$n = \dfrac{\nabla\phi}{\lvert \nabla \phi\rvert}$ is a unit normal vector
h	h is the grid size

ACKNOWLEDGEMENTS

On the completion of my dissertation, I would like to take this opportunity to thank my teachers, my family, and my friends

I especially appreciate the guidance of my advisor, Dr Songming Hou, for his constant encouragement and guidance during my Ph D program Dr Hou provided generous help to me both in my life and in research Without his precious advice and suggestions, I would not have today's achievement

I am also grateful to the teachers in the Department of Mathematics and Statistics, who gave me comprehensive knowledge during the past three academic years I also appreciate the feed-back from my dissertation committee members

My gratitude also goes to my beloved family Through these years, they have been standing behind me, sparing no effort to support me, giving me loving consideration and great confidence

Finally, but not lastly, I would like to thank my friends, especially Wei Wang, who gave me a lot of help to work out my problems during the difficult course of the dissertation, and encouraged me a lot in the three years of study here

CHAPTER 1

INTRODUCTION

1 1 Problems and Formulations

In the physical world, there are many problems whose solutions are separated by interfaces Determining the flow pattern of blood in the heart that is separated by heart valves, or finding the electric potential of a macromolecule that is infused into an ionic solvent (e g water) are two examples of such problems [7] This kind of problem is called an interface problem Interface problems have wide application in fluid dynamics, biomathematics, and material science among other fields

In this dissertation, the focus is on elliptic and elasticity interface problems For elliptic problems, the partial differential equation is

$$-\nabla \cdot (\beta(x) \nabla u(x)) = f(x), \quad x \in \Omega \setminus \Gamma, \tag{1 1}$$

with jump conditions

$$\begin{cases} [u]_\Gamma(x) \equiv u^+(x) - u^-(x) = a(x), \\ [(\beta \nabla u) \cdot n]_\Gamma(x) \equiv n \cdot (\beta^+(x) \nabla u^+(x)) - n \cdot (\beta^-(x) \nabla u^-(x)) = b(x), \end{cases} \tag{1 2}$$

and boundary conditions

$$u(x) = g(x), \quad x \in \partial\Omega \tag{1 3}$$

For elasticity problems, the partial differential equation is

$$\begin{cases} -\nabla \cdot (\beta_1(x)\nabla u_1(x)) - \nabla \cdot (\beta_2(x)\nabla u_2(x)) = f_1(x), \\ \\ -\nabla \cdot (\beta_3(x)\nabla u_1(x)) - \nabla \cdot (\beta_4(x)\nabla u_2(x)) = f_2(x), \end{cases} \quad x \in \Omega \setminus \Gamma, \tag{1.4}$$

with jump conditions

$$\begin{cases} [u_1]_\Gamma(x) \equiv u_1^+(x) - u_1^-(x) = a_1(x), \\ \\ [u_2]_\Gamma(x) \equiv u_2^+(x) - u_2^-(x) = a_2(x), \\ \\ n \cdot (\beta_1^+(x)\nabla u_1^+(x) + \beta_2^+(x)\nabla u_2^+(x)) - \\ n \cdot (\beta_1^-(x)\nabla u_1^-(x) + \beta_2^-(x)\nabla u_2^-(x)) = b_1(x), \\ \\ n \cdot (\beta_3^+(x)\nabla u_1^+(x) + \beta_4^+(x)\nabla u_2^+(x)) - \\ n \cdot (\beta_3^-(x)\nabla u_1^-(x) + \beta_4^-(x)\nabla u_2^-(x)) = b_2(x), \end{cases} \tag{1.5}$$

and boundary conditions

$$\begin{cases} u_1(x) = g_1(x), \\ \\ u_2(x) = g_2(x), \end{cases} \quad x \in \partial\Omega \tag{1.6}$$

In electrostatics, for example, β represents the dielectric coefficient. It is about 2 in a macromolecule, 80 in water. f represents the charge density. Solving the interface problem gives the electric potential u. In material science, u represents the potential or the pressure, and β is about 1 for air, $12 - 13$ for silicon. Usually, the balance laws across interfaces bring out the jump conditions [7].

Since an irregular domain can be embedded into a regular domain, the original boundary condition can be changed to jump conditions, and a boundary value problem for an irregular domain can be converted into an interface problem for a regular domain [7].

1 2 The Current Method

This dissertation further generalizes the method introduced in [15, 16] A finite element formulation was used to solve the elliptic and elasticity interface problems The theorems in [15] are generalized in this dissertation and proofs are provided It was also proved that the resulting linear system is (unsymmetric) positive definite if β is positive definite and lower-order terms are not present The numerical results show that this method is second-order accurate in the L^∞ norm for piecewise smooth solutions

The idea of solving elliptic and elasticity interface problems is shown in the following steps

(1) Set up the partition of the domain In two-dimensional models, the whole domain is cut into right triangles In three-dimensional models, the whole domain is cut into similar tetrahedrons

(2) On the interface cells, locate the end points of the interface segment In two dimensions, for the case of two domains, the interface segment is a straight line, for the case of three domains, the interface segment can either be one straight line or three straight lines connected at one point The interface segment is denoted by Γ_K^h In three dimensions, the interface segment would be a triangle or a polygon, and is denoted by Γ_L^h The locations of the interface segments can be calculated from the level-set function $\phi = \phi(x_i, y_j)$ The jump condition a is defined at these end points, and another jump condition b is defined at the center point of the interface segment

(3) Use the jump conditions a and b to calculate the numerical solution at end points on the interface segment For elliptic interface problems, the numerical solution at end points should be the linear combination of the jump condition values mentioned above and the values of interface cell vertices For elasticity interface problems, it is a little more complicated than the elliptic case Because there are two solutions defined on each interface cell, the number of jump conditions and the number of vertices would double

(4) Calculate the integration on the left hand side of Equations 1 1 and 1 4 on each cell For a regular cell, it would be easy to integrate because all the functions are supposed to be continuous on this cell For an interface cell, if it is separated into two different subdomains by the interface, the integration consists of two different functional integrations If the interface cell is separated into three different subdomains by the interfaces, the integration consists of three different functional integrations In order to make this method more accurate, the Gaussian quadrature rule is used for integration in this dissertation

(5) Set up the system matrix

(6) Calculate the integration on the right hand side of Equations 1 1 and 1 4 on each cell Use the same technique as above

(7) Solve the linear system of equations Because the system matrix is non-symmetric, the biconjugate gradient stabilized method is used in this dissertation

(8) Draw the figure and analyze the result

1 3 Outline of This Dissertation

The study of elliptic and elasticity interface problems has a long history In Chapter 2, the main previous work in this field is introduced

Chapter 3 builds on the method in [15] A more accurate finite element method is proposed to solve elliptic equations with sharp-edged interfaces with β being uniformly elliptic (therefore positive definite) and lower-order terms present Experimental results show that the order of accuracy for sharp-edged interfaces was improved from 0 8th to close to second order

In Chapter 4, the numerical method in [16] is extended to solve the elasticity problem with sharp-edged interfaces The method is simpler compared to that developed in [12] and it can be applied for more general problems since the β_i are allowed to be matrices Also, the proof of the positive definite property of the system matrix is provided, and numerical results are second-order accurate

Solving the elliptic problem with three domains is a new and challenging work In Chapter 5, this method is used to deal with three-domain problems The appearance of the triple junction point is a new challenge The method is extended and numerical results demonstrate near second-order accuracy for piecewise smooth solutions

In Chapter 6, this method is extended to solve the three-dimensional elliptic problem with two domains Three-dimensional problems are always more complicated,and solving it accurately would be a big challenge However, this method can deal with three dimensions simply and accurately All the results can achieve second-order accuracy

CHAPTER 2

PREVIOUS WORK

Although the importance of elliptic and elasticity interface problems has been well recognized in a variety of disciplines, designing highly efficient methods for these problems is a difficult job because of the low global regularity of the solution Since 1977, after the pioneering work of Peskin [30], much attention has been paid to the numerical solution of elliptic interface equations on regular Cartesian grids In many studies, simple Cartesian grids are preferred In this way, the complicated procedure of generating an unstructured grid can be bypassed, and well-developed fast algebraic solvers can be used

In [30, 31], in order to simulate the flow patten of blood in the heart, Peskin proposed the "immersed boundary" method, which used an improved numerical approximation of the δ-function In [32], in order to compute two-phase flow, a level-set method was combined with the "immersed boundary" method The level-set method was used to "capture" the interface between two fluids This method can get first-order accuracy even in multiple spatial dimensions

In [25, 26], the interface is smooth but irregular They extend the solution to a rectangular region by using Fredholm integral equations This equation can deal with interface conditions $[u] \neq 0$ and $[u_n] = 0$ The discrete Laplacian was evaluated using these jump conditions When a fast Poisson solver is used to compute the extended solution, it can achieve second or higher-order accuracy

In [6], second-order elliptic problems with two-dimensional convex polygonal domains are solved with a finite element method It can achieve second-order accuracy in the energy norm and nearly second-order accuracy in the L^2 norm when the interfaces are smooth but of arbitrary shape, and it can be extended to solve self-adjoint elliptic problems

The "immersed interface" method was proposed in [17] This method incorporates the interface conditions into the finite difference stencil, preserving that neither of the two jump conditions are zero It can get second-order accuracy The corresponding linear system is neither positive definite nor symmetric Various applications and extensions of the "immersed interface" method are provided in [21]

In [18], on the basis of the "immersed interface" method, a fast iterative method was proposed to solve constant coefficient problems with the interface conditions $[u] = 0$ and $[\beta u_n] \neq 0$ Before using the immersed interface method, the differential equation is preconditioned The discretization can guarantee second-order accuracy A GMRES iteration is used to solve the Schur complement system The number of iterations is independent of the jump in the coefficients and the mesh size

In [19, 20], the immersed finite element methods (IFEM) were developed using non-body-fitted Cartesian meshes for homogeneous jump conditions The idea is to modify the basis functions so that the homogeneous jump conditions are satisfied Both non-conforming and conforming IFEM were developed in [20] for two-dimensional problems

The boundary condition capturing method [22] was proposed on basis of the Ghost fluid method [10] Both methods are robust and simple to implement In [33], they improved the boundary condition capturing method with a multi-grid method The weak formulation provided in [23] was discretized to achieve this method Elliptic problems with interface conditions $[u] \neq 0$ and $[\beta u_n] \neq 0$ in two dimensions and three dimensions can be solved by this method However, the method in [22] can only get first-order accuracy It is in recent work [24] that for smooth interfaces the result was improved to second-order accuracy

In [14], a discontinuous Galerkin(DG) method is proposed to solve elliptic interface problems The matrix generated by this method is symmetric, and can be efficiently solved with standard algorithms Numerical experiments show that this method is optimally convergent in the L^2 norm for C^2 interfaces

In [15], a non-traditional finite element formulation for solving elliptic equations with smooth or sharp-edged interfaces was proposed with non-body-fitting grids for $[u] \neq 0$ and $[\beta u_n] \neq 0$ It achieved second-order accuracy in the L^∞ norm for smooth interfaces and about 0 8th order for sharp-edged interfaces In [40], the matched interface and boundary (MIB) method was proposed to solve elliptic equations with smooth interfaces In [39], the MIB method was generalized to treat sharp-edged interfaces In [38], the three-dimensional generalization of the MIB method was developed for solving elliptic equations with discontinuous coefficients and non-smooth interfaces In [34], they developed MIB method based schemes for solving two-dimensional elliptic PDEs with geometric singularities of multi-material interfaces With an elegant treatment, second-order accuracy was achieved in the L^∞ norm

However, for oscillatory solutions, the errors degenerated Also, there has been a large body of work from the finite volume perspective for developing high order methods for elliptic equations in complex domains, such as [8, 28] for two-dimensional problems and [29] for three-dimensional problems Another recent work in this area is a class of kernel-free boundary integral (KFBI) methods for solving elliptic BVPs, presented in [37]

There are some other approaches to solve the elliptic interface problems In particular, the recent work in [2] can handle sharp-edged interfaces However, these approaches have not been developed to solve elasticity interface problems Designing highly efficient methods for these problems is a difficult job, especially when the interface is not smooth

An elasticity system can be solved by both the finite difference and the finite element method Due to the cross derivative term, usually the linear system of equations using the finite element formulation is better conditioned compared with that obtained using a finite difference discretization

To solve the interface problem, first a mesh must be generated One approach is to use a body-fitted mesh coupled with a finite element discretization [1, 3, 4, 5] for scalar elliptic partial differential equations (PDEs) Recently, Cartesian meshes have become popular, especially for moving interface problems to overcome the cost in the grid generation at every or every other time step

Finite difference methods are proposed in [35, 36] with non-homogeneous jump conditions While second-order accuracy was achieved, the condition number of the discrete system is quite large, especially in the nearly incompressible case (λ is large) compared with that obtained from finite element formulations In [35, 36], a first-order immersed interface finite element method (IIFEM) was proposed using Cartesian meshes for the elasticity problem with homogeneous jump conditions In general, the discretization using a finite element discretization has a better conditioned system of equations compared with that obtained from the finite difference method The Soblev space theory provides strong theoretical foundations for convergence analysis of finite element methods

In [11], an immersed-interface finite element method was proposed for scalar elliptic interface problems with non-homogeneous jump conditions In [12], a class of new immersed-interface finite element methods (IIFEM) was proposed to solve elasticity interface problems with homogeneous and non-homogeneous jump conditions in two dimensions

CHAPTER 3

2-D ELLIPTIC PROBLEM WITH TWO DOMAINS

In this chapter, a finite element formulation is used to solve elliptic equations with sharp-edged interfaces with β being uniformly elliptic (therefore positive definite) and lower-order terms present The resulting linear system of equations is shown to be positive definite under certain assumptions Extensive numerical experiments are also provided Compared with the previous work in [15], the order of accuracy for sharp-edged interfaces is improved from 0 8th to close to second order Compared with the results in [39], the more oscillatory the solution is, the more advantageous the current method is The orders of accuracy for different regularities of solutions and different regularities of interfaces are listed in Table 3 11

3 1 Equations and Weak Formulations

Let $\Omega \subset R^d$ be an open bounded domain and let Γ be an interface Γ divides Ω into two disjoint open subdomains Ω^- and Ω^+, $\Omega = \Omega^- \bigcup \Omega^+ \bigcup \Gamma$ Let $\partial\Omega$ be the boundary of Ω, $\partial\Omega^\pm$ be the boundary of each subdomain We assume that $\partial\Omega$ and $\partial\Omega^\pm$ are Lipschitz continuous and so is Γ A unit normal vector of Γ can be defined almost everywhere on Γ

The variable coefficient elliptic interface problem is given by

$$-\nabla\cdot(\beta(x)\nabla u(x)) + p(x)\cdot\nabla u(x) + q(x)u(x) = f(x), \quad x \in \Omega\setminus\Gamma, \tag{3.1}$$

where $x = (x_1, \ldots, x_d)$ are the spatial variables. $\beta(x)$ is defined to be a $d\times d$ matrix that is uniformly elliptic on Ω^- and Ω^+, and its components are continuously differentiable on Ω^- and Ω^+, but they might be discontinuous across Γ. $f(x)$ is in $L^2(\Omega)$.

The jump conditions are prescribed

$$\begin{cases} [u]_\Gamma(x) \equiv u^+(x) - u^-(x) = a(x), \\ [(\beta\nabla u)\cdot n]_\Gamma(x) \equiv n\cdot(\beta^+(x)\nabla u^+(x)) - n\cdot(\beta^-(x)\nabla u^-(x)) = b(x), \end{cases} \tag{3.2}$$

a and b are given functions along the interface Γ, " $\pm$ " denote limits taken within $\Omega^\pm$.

The boundary conditions are prescribed by a function g, given on $\partial\Omega$.

$$u(x) = g(x), \quad x \in \partial\Omega. \tag{3.3}$$

The weak formulation in [15] is generalized for the elliptic equation with matrix coefficients and lower-order terms present. The usual Sobolev space $H^1(\Omega)$ is used. For $H_0^1(\Omega)$, an inner product is chosen as

$$\begin{gathered} B[u,v] = \int_{\Omega^+}\beta\nabla u\cdot\nabla v + \int_{\Omega^-}\beta\nabla u\cdot\nabla v + \\ \int_{\Omega^+}(p\cdot\nabla u)v + \int_{\Omega^-}(p\cdot\nabla u)v + \int_{\Omega^+}quv + \int_{\Omega^-}quv \end{gathered} \tag{3.4}$$

Remark 1 For general second-order elliptic equations with lower-order p, q terms, one of the hypotheses of the Lax-Milgram Theorem is not guaranteed. For detailed discussion about the energy estimates and a first existence theorem for weak solutions, see [9] Although a numerical example with $p \neq 0$, $q \neq 0$ in Section 3 3 is provided, for ease of theoretical discussion, it is assumed that $p = 0$, $q = 0$ for the rest of this section as well as in Section 3 2

Equation 3 4 without the p, q terms induces a norm on $H_0^1(\Omega)$, which is equivalent to the usual one, thanks to the Poincare inequality and the uniformly ellipticity and boundedness of $\beta(x)$ on Ω

Let R be the restriction operator from $H^1(\Omega)$ to $L^2(\partial\Omega^-)$ R is closed Lipschitz continuous (see Theorem 2 4 2 in [27]) on $C^1(\overline{\Omega})$ and because $C^1(\overline{\Omega})$ is dense in $H^1(\Omega)$, it is well defined and bounded For functions $\widetilde{a}, \widetilde{b} \in H^1(\Omega)$, the restrictions to $\partial\Omega^-$ are

$$a = R_{\partial\Omega^-}(\widetilde{a}), b = R_{\partial\Omega^-}(\widetilde{b}) \tag{3 5}$$

Throughout, we assume a function $\widetilde{c} \in H^1(\Omega)$ exists so that the boundary condition on $\partial\Omega$ is

$$g = \begin{cases} R_{\partial\Omega}(\tilde{c} - \tilde{a}), \text{on } \partial\Omega \bigcap \partial\Omega^-, \\ R_{\partial\Omega}(\tilde{c}), \text{on } \partial\Omega \backslash \partial\Omega^- \end{cases} \tag{3 6}$$

For simplicity, the tildes are dropped in this dissertation

A unique solution of the problem is constructed in the space

$$H(a, c) = \{u \quad u - c + a\chi(\overline{\Omega^-}) \in H_0^1(\Omega)\} \tag{3 7}$$

If $u \in H(a, c)$, then $[u]_\Gamma = a$, $u|_{\partial\Omega} = g$ $H_0^1(\Omega)$ can be written as $H(0,0)$ A similar idea is also used in [15, 16]

Definition 3 1 1 $u \in H(a,c)$ is called a weak solution of Equations 3 1-3 3, if $v = u - c + a\chi(\overline{\Omega^-}) \in H_0^1(\Omega)$ satisfies

$$B[v,\psi] = F(\psi), \tag{3 8}$$

for all $\psi \in H_0^1(\Omega)$, where

$$B[v,\psi] = \int_{\Omega^+} \beta \nabla v \;\; \nabla\psi + \int_{\Omega^-} \beta \nabla v \;\; \nabla\psi, \tag{3 9}$$

$$F(\psi) = \int_{\Omega} f\psi + \int_{\Omega} \beta \nabla c \;\; \nabla\psi + \int_{\Omega^-} \beta \nabla a \;\; \nabla\psi + \int_{\Gamma} b\psi \tag{3 10}$$

Or equivalently

Definition 3 1 2 $u \in H(a,c)$ is called a weak solution of Equations 3 1-3 3, if it satisfies, for all $\psi \in H_0^1(\Omega)$,

$$\int_{\Omega^+} \beta \nabla u \;\; \nabla\psi + \int_{\Omega^-} \beta \nabla u \;\; \nabla\psi = \int_{\Omega} f\psi + \int_{\Gamma} b\psi \tag{3 11}$$

Theorem 3 1 3 If $f \in L^2(\Omega)$, and a, b, $c \in H^1(\Omega)$, then there exists a unique weak solution of Equations 3 1-3 3 in $H(a,c)$

Proof See Theorem 2 1 in [15] □

3 2 Numerical Method

For simplicity, assume a, b and c are smooth on $\overline{\Omega}$ β and f are smooth on Ω^+ and Ω^-, but might be discontinuous across Γ $\partial\Omega$, $\partial\Omega^-$ and $\partial\Omega^+$ are Lipschitz continuous ϕ is a level-set function on Ω, where $\Gamma = \{\phi = 0\}$, $\Omega^- = \{\phi < 0\}$ and $\Omega^+ = \{\phi > 0\}$ $n = \frac{\nabla\phi}{|\nabla\phi|}$ is a unit normal vector of Γ pointing from Ω^- to Ω^+

The setup is restricted to a rectangular domain $\Omega = (x_{min}, x_{max}) \times (y_{min}, y_{max})$ in the plane, and β is a 2×2 matrix that is uniformly elliptic in each subdomain Let I

and J be positive integers, set $\Delta x = (x_{max} - x_{min})/I$ and $\Delta y = (y_{max} - y_{min})/J$ A uniform Cartesian grid is defined as $(x_i, y_j) = (x_{min} + i\Delta x, y_{min} + j\Delta y)$ for $i = 0, \quad , I$ and $j = 0, \quad , J$ $h = max(\Delta x, \Delta y) > 0$ is the grid size

Two grid function sets will be used

$$H^{1,h} \quad = \quad \{\omega^h = (\omega_{i,j}) \quad 0 \leq i \leq I, 0 \leq j \leq J\},$$

and

$$H_0^{1,h} \quad = \quad \{\omega^h = (\omega_{i,j}) \in H^{1,h} \quad \omega_{i,j} = 0 \text{ if } i = 0, I \text{ or } j = 0, J\}$$

Every rectangular region $[x_i, x_{i+1}] \times [y_j, y_{j+1}]$ is cut into two right triangular regions When all those triangular regions are collected, a uniform triangulation $T^h \quad \bigcup_{K \in T^h} K$ is obtained, see Figure 3 1

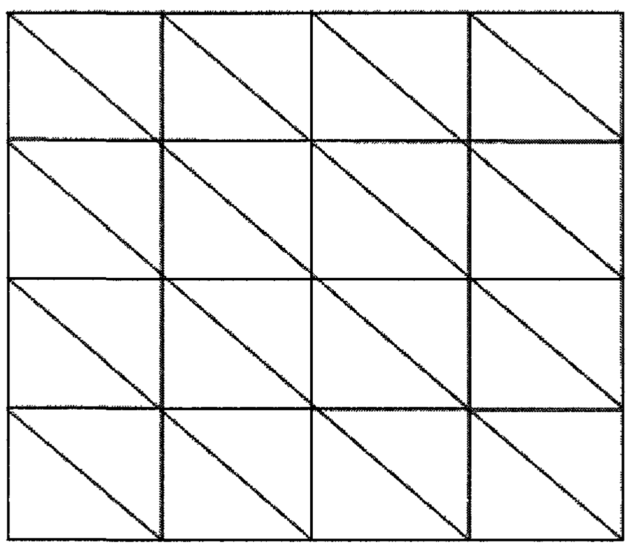

Figure 3 1 A uniform triangulation

If $\phi(x_i, y_j) \leq 0$, the grid point (x_i, y_j) is counted as in $\overline{\Omega^-}$, otherwise it is counted as in Ω^+

A cell $\triangle_k$ with corners k_1, k_2, k_3 belongs to one of two different sets

$$\Lambda_1 = \{\triangle_k \subset \Omega \quad k_1, k_2, k_3 \text{ are in the same domain among } \Omega^{\pm}\},$$

$$\Lambda_2 = \{\triangle_k \subset \Omega \quad k_1, k_2, k_3 \text{ are in two different domains among } \Omega^{\pm}\}$$

If a cell belongs to Λ_1, it is a regular cell, otherwise, it is an interface cell The interface segment Γ^h_K separates the interface cell into K^+ and K^-

In this dissertation, two extension operators are needed

T^h $H^{1,h} \to H^1_0(\Omega)$ For any $\psi^h \in H^{1,h}_0$, $T^h(\psi^h)$ is a standard continuous piecewise linear function in every triangular cell matching ψ^h on grid points The function set is a subspace of $H^1_0(\Omega)$, which can be written as $H^{1,h}_0$

U^h For any $u^h \in H^{1,h}$, $u^h = g^h$ at boundary points, $U^h(u^h)$ is a piecewise linear function in every triangular cell matching u^h on grid points In a regular cell, $U^h(u^h) = T^h(u^h)$ is a linear function In an interface cell, $U^h(u^h)$ is one linear function on K^+ and another linear function on K^- A similar extension is also used in [15, 16, 20, 22] In order to use this extension, the following theorem is needed

Theorem 3 2 1 For all $u^h \in H^{1,h}, U^h(u^h)$ can be constructed uniquely, if T^h, ϕ, a and b are given

Proof There are three typical cases for $U^h(u^h)$

Case 0 As is shown in Figure 3 2, if K is a regular cell, $U^h(u^h) = T^h(u^h)$, i e

$$U^h(u^h) = u(p_1) + \frac{u(p_2) - u(p_1)}{\Delta x}(x - x_i) + \frac{u(p_3) - u(p_1)}{\Delta y}(y - y_i) \qquad (3\ 12)$$

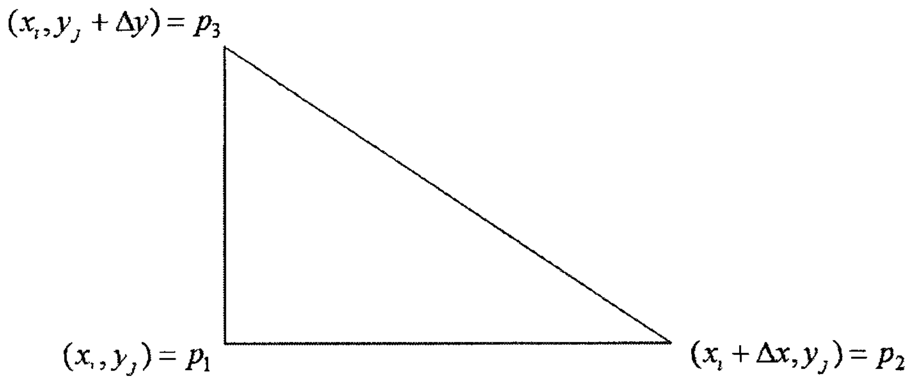

Figure 3 2 The regular cell

Case 1 As is shown in Figure 3 3, if K is an interface cell with Γ cuting through two legs of K, then

$$U^h(u^h) = \begin{cases} u(p_1) + u_x^+(x - x_i) + u_y^+(y - y_i) & (x,y) \in K^+, \\ u(p_2) + u_x^-(x - x_i - \triangle x) + u_y^-(y - y_i) & (x,y) \in K^-, \end{cases} \tag{3 13}$$

here $u_y^- = \frac{u(p_3) - u(p_2)}{\triangle y} + \frac{\triangle x}{\triangle y} u_x^-$,

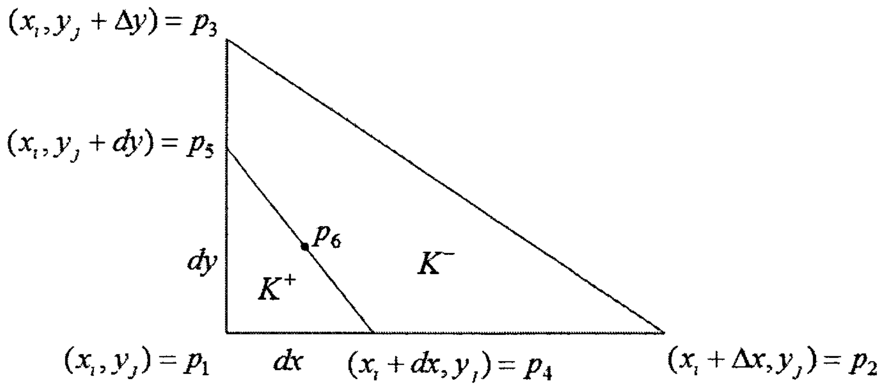

Figure 3 3 The interface cell Case 1

In Figure 3 3, $\vec{n} = (-\frac{dy}{\sqrt{dx^2+dy^2}}, -\frac{dx}{\sqrt{dx^2+dy^2}})$

$$\begin{cases} u_x^+ = \frac{u(p_4)+a-u(p_1)}{dx}, \\ u_y^+ = \frac{u(p_5)+a-u(p_1)}{dy} \end{cases} \tag{3 14}$$

In Figure 3 4, it is assumed that the extensions of p_3p_5 and p_2p_4 intersect at a ghost point called p_1^G, therefore

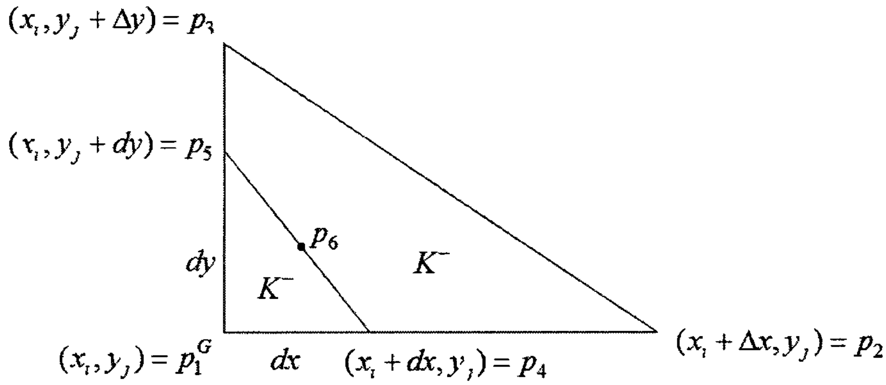

Figure 3 4 The ghost point

$$\begin{cases} \frac{u(p_1^G)-u(p_4)}{dx} = \frac{u(p_4)-u(p_2)}{\Delta x - dx}, \\ \frac{u(p_1^G)-u(p_5)}{dy} = \frac{u(p_1^G)-u(p_3)}{\Delta y}, \end{cases} \tag{3 15}$$

and

$$\begin{cases} u_x^- = \frac{u(p_2)-u(p_4)}{\Delta x - dx}, \\ u_y^- = \frac{u(p_3)-u(p_5)}{\Delta y - dy} \end{cases} \tag{3 16}$$

From Equation 3 15 and Equation 3 16

$$u(p_1^G) = \frac{dx}{\Delta x - dx}(u(p_4) - u(p_2)) + u(p_4), \tag{3 17}$$

$$u(p_5) = u(p_1^G) - \frac{dy}{\Delta y}(u(p_1^G) - u(p_3)) \tag{3 18}$$

Let

$$\beta = \begin{pmatrix} \beta_{11} & \beta_{12} \\ \beta_{21} & \beta_{22} \end{pmatrix} \tag{3 19}$$

From Equations 3 14-3 19, note that u_x^-, u_y^-, u_x^+ and u_y^+ can all be written as linear functions of $u(p_1), u(p_2), u(p_3)$ and $u(p_4)$ Since $b = \beta \bigtriangledown u \quad \vec{n}$, then

$$\begin{aligned} b &= \beta^+ \bigtriangledown u^+ \quad \vec{n} - \beta^- \bigtriangledown u^- \quad \vec{n} \\ &= \beta_{11}^+ u_x^+ n_1 + \beta_{12}^+ u_y^+ n_1 + \beta_{21}^+ u_x^+ n_2 + \beta_{22}^+ u_y^+ n_2 - \\ &\quad (\beta_{11}^- u_x^- n_1 + \beta_{12}^- u_y^- n_1 + \beta_{21}^- u_x^- n_2 + \beta_{22}^- u_y^- n_2) \end{aligned} \tag{3 20}$$

From Equations 3 14-3 20, the value of $u(p_4)$ can be obtained It is a linear function of $u(p_1), u(p_2), u(p_3)$ Hence u_x^-, u_y^-, u_x^+ and u_y^+ can be written in the following form

$$\begin{cases} u_x^+ = c_{x,1}^+ u(p_1) + c_{x,2}^+ u(p_2) + c_{x,3}^+ u(p_3) + c_{x,4}^+ a(p_4) + c_{x,5}^+ a(p_5) + c_{x,6}^+ b(p_6), \\ u_y^+ = c_{y,1}^+ u(p_1) + c_{y,2}^+ u(p_2) + c_{y,3}^+ u(p_3) + c_{y,4}^+ a(p_4) + c_{y,5}^+ a(p_5) + c_{y,6}^+ b(p_6), \\ u_x^- = c_{x,1}^- u(p_1) + c_{x,2}^- u(p_2) + c_{x,3}^- u(p_3) + c_{x,4}^- a(p_4) + c_{x,5}^- a(p_5) + c_{x,6}^- b(p_6), \\ u_y^- = c_{y,1}^- u(p_1) + c_{y,2}^- u(p_2) + c_{y,3}^- u(p_3) + c_{y,4}^- a(p_4) + c_{y,5}^- a(p_5) + c_{y,6}^- b(p_6) \end{cases} \tag{3 21}$$

To complete the proof for Case 1, the following lemma is needed

Lemma 3 2 2 All coefficients c in Equation 3 21 are independent of u^h, a and b

For simplicity, $c_{x,3}^+$ is taken as an example The claim for the other coefficients can be proved similarly

$$c_{x,3}^+ = \alpha[-(\beta_{12}^+ dy + \beta_{22}^+ dx)dy(\triangle x - dx) + (\beta_{12}^- dy + \beta_{22}^- dx)dy(\triangle x - dx)], \tag{3 22}$$

where $\frac{1}{\alpha} = (\beta_{11}^+ dy + \beta_{21}^+ dx) \triangle y(\triangle x - dx)dy + (\beta_{12}^+ dy + \beta_{22}^+ dx) \triangle x(\triangle y - dy)dx$
$+ (\beta_{11}^- dy + \beta_{21}^- dx) \triangle ydxdy + (\beta_{12}^- dy + \beta_{22}^- dx) \triangle xdxdy$

From Equation 3 22, it is easy to tell that $c^+_{x,3}$ is independent of u^h, a and b

Case 2 As is shown in Figure 3 5, if K is an interface cell with Γ cutting through the hypotenuse and one leg of K, then

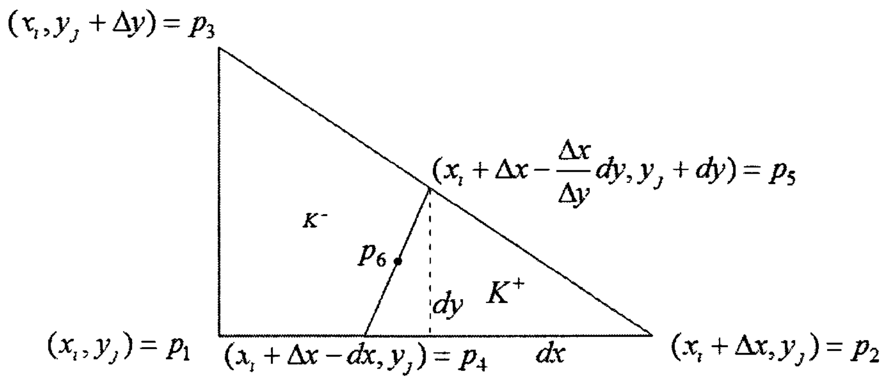

Figure 3 5 The interface cell Case 2

$$U^h(u^h) = \begin{cases} u(p_2) + u^+_x(x - x_i - \Delta x) + u^+_y(y - y_i) & (x, y) \in K^+, \\ u(p_1) + u^-_x(x - x_i) + \frac{u(p_3) - u(p_1)}{\Delta y}(y - y_i) & (x, y) \in K^- \end{cases} \tag{3 23}$$

Similar derivation as in Case 1 gives

$$\begin{cases} u^+_x = d^+_{x,1}u(p_1) + d^+_{x,2}u(p_2) + d^+_{x,3}u(p_3) + d^+_{x,4}a(p_4) + d^+_{x,5}a(p_5) + d^+_{x,6}b(p_6), \\ u^+_y = d^+_{y,1}u(p_1) + d^+_{y,2}u(p_2) + d^+_{y,3}u(p_3) + d^+_{y,4}a(p_4) + d^+_{y,5}a(p_5) + d^+_{y,6}b(p_6), \\ u^-_x = d^-_{x,1}u(p_1) + d^-_{x,2}u(p_2) + d^-_{x,3}u(p_3) + d^-_{x,4}a(p_4) + d^-_{x,5}a(p_5) + d^-_{x,6}b(p_6), \\ u^-_y = d^-_{y,1}u(p_1) + d^-_{y,2}u(p_2) + d^-_{y,3}u(p_3) + d^-_{y,4}a(p_4) + d^-_{y,5}a(p_5) + d^-_{y,6}b(p_6) \end{cases} \tag{3 24}$$

To complete the proof for Case 2, the following lemma is needed

Lemma 3 2 3 All coefficients d in Equation 3 24 are independent of u^h, a and b

Same idea as Lemma 3 2 2, details are skipped here

Therefore, Theorem 3 2 1 has been completely proved □

Based on the above discussion, the following method is proposed

Method 1 Find a discrete function $u^h \in H^{1,h}$ such that $u^h = g^h$ on the boundary points and so that for all $\psi^h \in H_0^{1,h}$, there is

$$\sum_{K \in T^h} \left(\int_{K^+} \beta \nabla U^h(u^h) \cdot \nabla T^h(\psi^h) + \int_{K^-} \beta \nabla U^h(u^h) \cdot \nabla T^h(\psi^h) \right)$$
$$= \sum_{K \in T^h} \left(\int_{K^+} f T^h(\psi^h) + \int_{K^-} f T^h(\psi^h) + \int_{\Gamma_K^h} b T^h(\psi^h) \right) \qquad (3.25)$$

On the boundary $u = g$ is equivalent to $u - c + a\chi(\overline{\Omega^-}) = 0$.

For the general case with $p \neq 0, q \neq 0$, the integral for these lower-order terms could be added to the above weak formulation.

To implement the above method, the Gaussian quadrature rule for integrals is used. The idea is illustrated in Figure 3.6. If T is separated into two pieces by the interface $\overline{u_4 u_5}$, u_3 and u_4 are connected, then three triangles are the result: $T_1 = \triangle u_1 u_4 u_5$, and $T_2 = \triangle u_2 u_3 u_4$, $T_3 = \triangle u_3 u_4 u_5$. For each triangle, the center point p_{ij} is labeled for each edge $\overline{u_i u_j}$. In numerical computation, the average of three $f(p_{ij})$ is applied in each triangle. Numerical results show an improvement over [15], where fewer sample points were used.

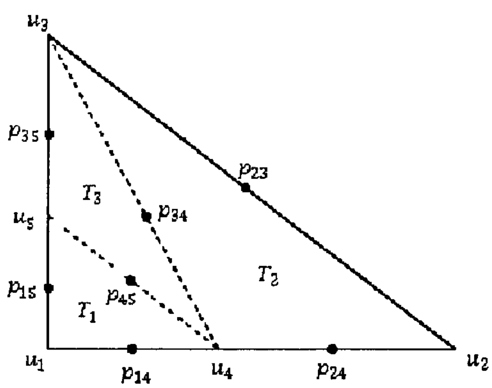

Figure 3.6 Quadrature rule

Since the solution bases and test function bases are different, the matrix A for the linear system generated by Method 1 is not symmetric in the presence of an interface However, it can be proved that it is positive definite

Theorem 3 2 4 If β is positive definite, and $p = q = 0$, then the $n \times n$ matrix A for the linear system generated by Method 1 is positive definite

Proof For any vector $c \in R^n$,

$$c^T A c = \sum_{i,j=1}^{n} a_{ij} c_i c_j = B\left[\sum_{i=1}^{n} c_i u^i, \sum_{i=1}^{n} c_i \psi^i\right],$$

where u^i and ψ^i are basis functions for the solution and the test function, respectively Note that they have compact support and have nonzero values only inside the six triangles around the ith grid point For ease of discussion, each of u^i and ψ^i is decomposed into six parts, so that each part has nonzero values only inside one triangle Now the summation over i is equivalent to a summation over all the triangles, and there are three terms, $c_1u_1+c_2u_2+c_3u_3$, $c_1\psi_1+c_2\psi_2+c_3\psi_3$ for each triangle, where $u_1, u_2, u_3, \psi_1, \psi_2, \psi_3$ equals 1 on one vertex of a triangle and zero on two other vertices The difference between u_i and ψ_i is, u_i depends on the location of the interface and ψ_i does not $c_1u_1 + c_2u_2 + c_3u_3$ is a piecewise linear function satisfying the jump conditions, and $c_1\psi_1 + c_2\psi_2 + c_3\psi_3$ is a linear function At the three vertices, the two functions coincide Now the jump conditions can be set at $a = 0$ and b can be set to have the value in the triangle such that $c_1u_1 + c_2u_2 + c_3u_3 = c_1\psi_1 + c_2\psi_2 + c_3\psi_3$ everywhere In other words, compensation is made for the jump in β by using b to make sure the gradients on both sides of the interface coincide Since Lemma 3 2 2 and Lemma 3 2 3 imply that the matrix A is independent of a, b, choosing the above

a, b would not change the matrix A and would only change the constant term, i e , the right hand side of the linear system Now the triangles are summed overall and the result is

$$\sum_{i=1}^{n} c_i u^i = \sum_{i=1}^{n} c_i \psi^i$$

It now follows from the positive definiteness of β that

$$c^T A c = B\left[\sum_{i=1}^{n} c_i u^i, \sum_{i=1}^{n} c_i u^i\right] > 0$$

Therefore A is positive definite □

Remark 2 A positive definite matrix A has positive determinant, and is therefore invertible It also has an LDM^T factorization where $D = diag(d_i)$ and $d_i > 0$, and L, M are lower triangular The linear system $Ax = b$ can be solved efficiently

Remark 3 For ease of discussion, both the p, q terms have been dropped However, the Lax-Milgram Theorem, the current Theorem 3 1 3, and Theorem 3 2 4 work for the case $p = 0$ and $q > 0$ as well For the case with nonzero p or negative q, the positive definiteness of A is no longer guaranteed, nor is one of the hypotheses of the Lax-Milgram Theroem

3 3 Numerical Experiments

Consider the problem

$$-\nabla \ (\beta\nabla u) + p \ \nabla u + qu = f, \text{ in } \Omega^{\pm}, \tag{3 26}$$

$$[u] = a, \text{ on } \Gamma, \tag{3 27}$$

$$[(\beta\nabla u) \ n] = b, \text{ on } \Gamma, \tag{3 28}$$

$$u = g, \text{ on } \partial\Omega, \tag{3 29}$$

on the rectangular domain $\Omega = (x_{min}, x_{max}) \times (y_{min}, y_{max})$ The interface Γ is prescribed by a level-set function $\phi(x, y)$ $n = \frac{\nabla\phi}{|\nabla\phi|}$ is the unit normal vector of Γ pointing from Ω^- to Ω^+

In all examples of this section, given $\phi(x, y)$, $\beta^{\pm}(x, y)$, $p^{\pm}(x, y)$, $q^{\pm}(x, y)$ and

$$u = u^+(x, y), \text{ in } \Omega^+, \tag{3 30}$$

$$u = u^-(x, y), \text{ in } \Omega^- \tag{3 31}$$

Hence

$$f = -\nabla \cdot (\beta\nabla u) + p \cdot \nabla u + qu, \tag{3 32}$$

$$a = u^+ - u^-, \tag{3 33}$$

$$b = (\beta^+\nabla u^+) \cdot n - (\beta^-\nabla u^-) \cdot n, \tag{3 34}$$

on Ω g is obtained from the given solutions as a proper Dirichlet boundary condition

All errors in solutions are measured in the L^∞ norm in the whole domain Ω All errors in the gradients of solutions are measured in the L^∞ norm away from interfaces

For Examples 1, 2, 3 and 4, let $p(x, y) = q(x, y) = 0$ and let $\beta^{\pm}$ be scalars Method 1 was implemented For Example 6, $\beta^{\pm}$ are symmetric positive definite matrices, and Method 1 was modified by adding the integrals for lower-order p, q terms As discussed in Section 3 1, in this general case, one of the hypotheses of the Lax-Milgram Theorem is not guaranteed However, since the true solution was constructed first, the existence of a weak solution is automatically guaranteed The numerical result is promising

Example 1 This example is taken from [39] ϕ, $\beta^{\pm}$ are

$$\phi(r,\theta) = \frac{R\sin(\theta_t/2)}{\sin(\theta_t/2+\theta-\theta_r-2\pi(i-1)/5)} - r$$

$$\theta_r + \pi(2i-2)/5 \le \theta < \theta_r + \pi(2i-1)/5, \quad (3\ 35)$$

$$\phi(r,\theta) = \frac{R\sin(\theta_t/2)}{\sin(\theta_t/2-\theta+\theta_r-2\pi(i-1)/5)} - r$$

$$\theta_r + \pi(2i-3)/5 \le \theta < \theta_r + \pi(2i-2)/5, \quad (3\ 36)$$

with $\theta_t = \pi/5,\ \theta_r = \pi/7,\ R = 6/7$ and $i = 1,2,3,4,5$

$$\beta^+(x,y) = 1, \quad (3\ 37)$$

$$\beta^-(x,y) = 2+\sin(x+y) \quad (3\ 38)$$

When the solutions $u^{\pm}$ are given as

$$u^+(x,y) = 5+5(x^2+y^2), \quad (3\ 39)$$

$$u^-(x,y) = x^2+y^2+\sin(x+y) \quad (3\ 40)$$

The computed solution with the current method using a 40×40 grid is shown in Figure 3 7

When the solutions $u^{\pm}$ are given as

$$u^+(x,y) = 6+\sin(2\pi x)\sin(2\pi y), \quad (3\ 41)$$

$$u^-(x,y) = x^2+y^2+\sin(x+y) \quad (3\ 42)$$

The computed solution with the current method using a 40×40 grid is shown in Figure 3 8

When the solutions $u^{\pm}$ are given as

$$u^+(x,y) = 6+\sin(6\pi x)\sin(6\pi y), \quad (3\ 43)$$

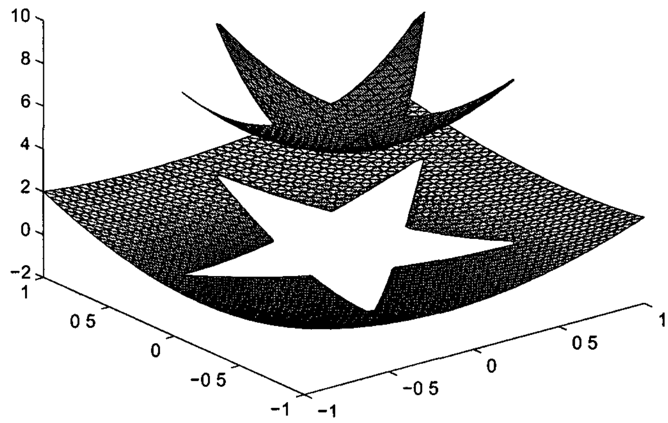

Figure 3 7 Star shape interface Case a

$$u^-(x, y) = x^2 + y^2 + \sin(x + y) \tag{3 44}$$

The computed solution with the current method using a 40×40 grid is shown in Figure 3 9 Table 3 1 shows the error of these three cases with the current method on different grids Table 3 2 shows the error of these three cases using the method in [39] on different grids These two tables show that as the solution gets more oscillatory, the current method is superior as better results were obtained than those presented in Table 3 2

Example 2 This example comes from [22] $\phi(x, y)$, $\beta^{\pm}(x, y)$ and $u^{\pm}(x, y)$ are

$$\phi(x, y) = x^2 + y^2 - 0\ 25, \tag{3 45}$$

$$\beta^+(x, y) = 1, \tag{3 46}$$

$$\beta^-(x, y) = 1, \tag{3 47}$$

$$u^+(x, y) = 0, \tag{3 48}$$

$$u^-(x, y) = exp(x)\cos(y) \tag{3 49}$$

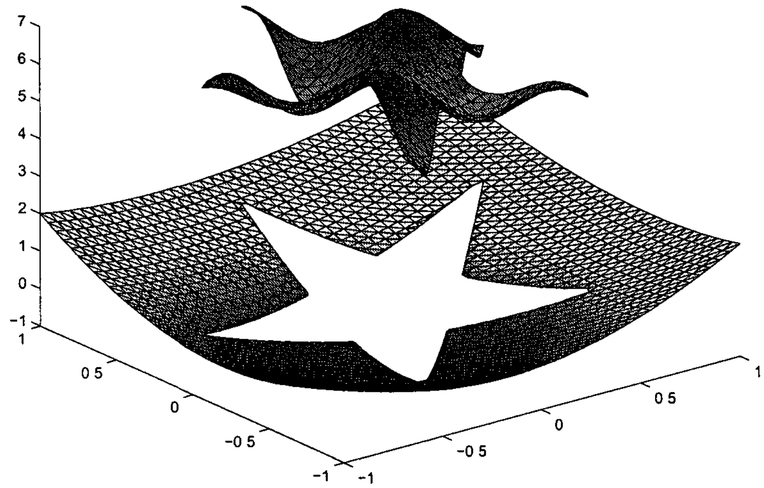

Figure 3 8 Star shape interface Case b

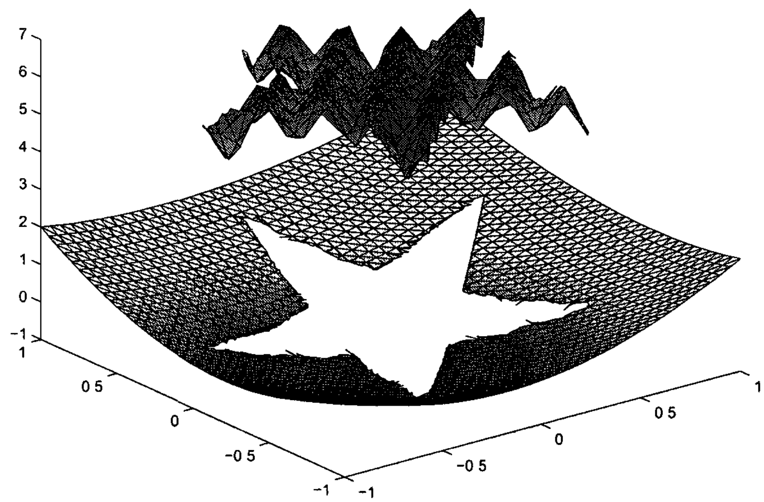

Figure 3 9 Star shape interface Case c

Figure 3 10 shows the computed solution with the current method using a 40×40 grid Table 3 3 shows the error on different grids for the new developed method and the method in [22] Comparing the results, it is easy to see that the method in [22] is first-order accurate, while the new developed method in this dissertation is second-order accurate

Table 3 1 Star Results of the new developed method

	Case(a)		Case(b)		Case(c)	
$n_x \times n_y$	Error in U	Order	Error in U	Order	Error in U	Order
20×20	7 70e-3		4 05e-2		3 40e-1	
40×40	1 76e-3	2 13	1 06e-2	1 94	8 88e-2	1 94
80×80	5 49e-4	1 68	2 50e-3	2 08	2 33e-2	1 93
160×160	1 41e-4	1 96	6 31e-4	1 98	5 68e-3	2 04

Table 3 2 Star Results using the method described in [39]

	Case(a)		Case(b)		Case(c)	
$n_x \times n_y$	Error in U	Order	Error in U	Order	Error in U	Order
20×20	6 11e-4		5 26e-2		9 72e-1	
40×40	6 07e-5	3 33	8 51e-3	2 62	1 94e-2	2 32
80×80	1 34e-5	2 18	2 39e-3	1 83	5 49e-2	1 82
160×160	4 15e-6	1 69	6 64e-4	1 85	1 48e-2	1 89

Example 3 This example comes from [17] $\phi(x,y)$, $\beta^{\pm}(x,y)$ and $u^{\pm}(x,y)$ are

$$\phi(x,y) = x^2 + y^2 - 0\ 25, \tag{3 50}$$

$$\beta^{+}(x,y) = 1, \tag{3 51}$$

$$\beta^{-}(x,y) = 1, \tag{3 52}$$

$$u^{+}(x,y) = 1 + \log(2\sqrt{x^2 + y^2}), \tag{3 53}$$

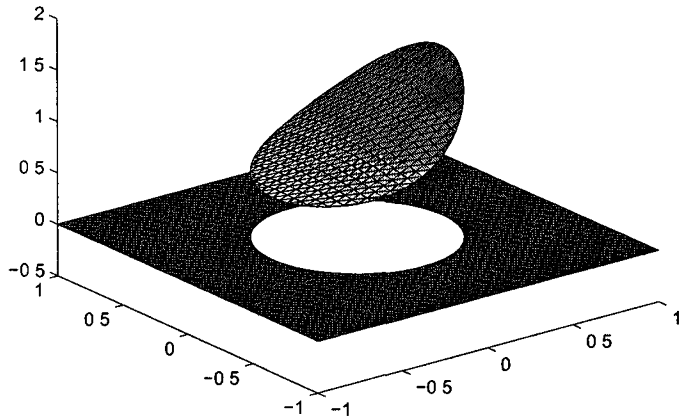

Figure 3 10 Example taken from [22]

Table 3 3 Example taken from [22]

Method	The new developed Method		Method in [22]	
$n_x \times n_y$	Error in U	Order	Error in U	Order
20×20	8 9972e-4		0 0153	
40×40	2 4524e-4	1 8753	0 0081	0 92
80×80	6 0982e-5	2 0077	0 0044	0 88
160×160	1 2886e-5	2 2425	0 0023	0 94

$$u^{-}(x, y) = 1 \tag{3 54}$$

Figure 3 11 shows the computed solution with the current method using a 40×40 grid Table 3 4 shows the error on different grids for the new developed method and the method in [17] Because the interface is smooth, both of these two methods can get to second-order accuracy

Example 4 This example is from [15] $\phi(x, y)$, $\beta^{\pm}(x, y)$ and $u^{\pm}(x, y)$ are

$$\phi(x,y) = (\sin(5\pi x) - y)(-\sin(5\pi y) - x), \tag{3 55}$$

$$\beta^+(x,y) = xy + 2, \tag{3 56}$$

$$\beta^-(x,y) = x^2 - y^2 + 3, \tag{3 57}$$

$$u^+(x,y) = 4 - x^2 - y^2, \tag{3 58}$$

$$u^-(x,y) = x^2 + y^2 \tag{3 59}$$

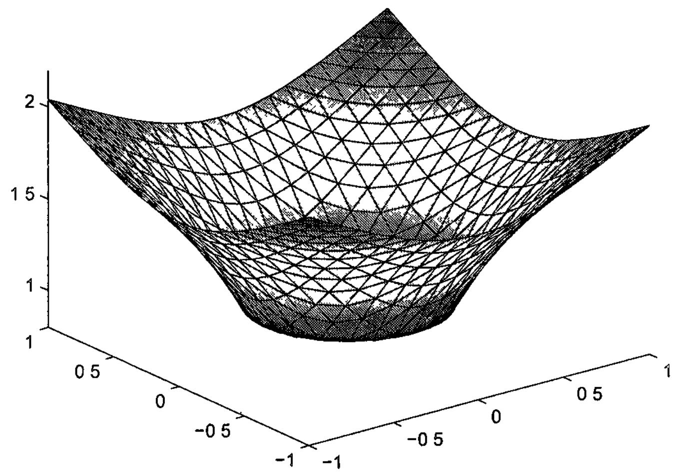

Figure 3 11 Example taken from [17]

The computed solution with the current method using a 40×40 grid is shown in Figure 3 12 Table 3 5 shows the error on different grids Compared with the results of [15], shown in Table 3 6, the current solution is more accurate than the previous work due to the quadrature rule discussed in Section 3 2

Example 5 is taken from [15] This example is used to investigate the order of the error in u and ∇u on solutions and interfaces with different regularity

Table 3 4 Example taken from [17]

Method	The new developed Method		Method in [17]	
$n_x \times n_y$	Error in U	Order	Error in U	Order
20×20	3 2039e-3		2 3908e-3	
40×40	8 8536e-4	1 8555	8 3461e-4	1 5183
80×80	2 3700e-4	1 9014	2 4451e-4	1 7712
160×160	5 8734e-5	2 0126	6 6856e-5	1 8708

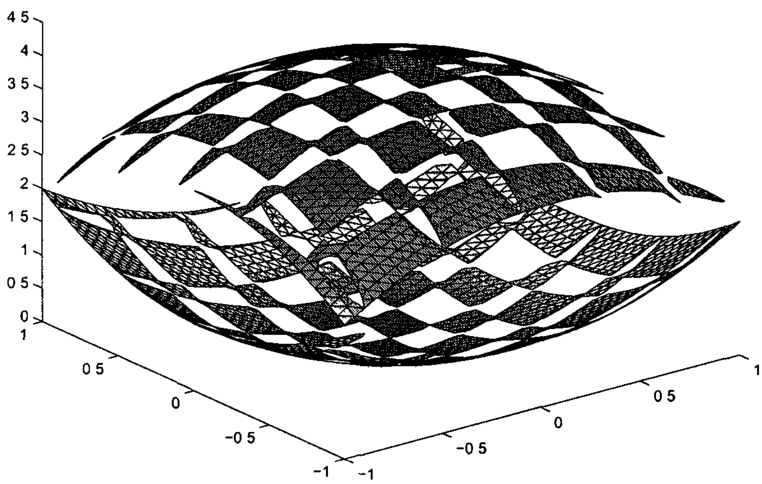

Figure 3 12 Interface with the shape of a chess board

Example 5 $\phi(x,y)$, $\beta^{\pm}(x,y)$ and $u^{\pm}(x,y)$ are given as follows The interface is Lipschitz continuous but has a sharp corner at $(0,0)$, u is piecewise H^2

$$\phi(x,y) = y - 2x, \; x+y > 0, \tag{3 60}$$

$$\phi(x,y) = y + x/2, \; x+y \leq 0, \tag{3 61}$$

$$\beta^{+}(x,y) = 1, \tag{3 62}$$

Table 3 5 Chess board Results of the new developed method

$n_x \times n_y$	Error in U	Order	Error in ∇U	Order
40×40	9 74e-4		4 650e-3	
80×80	2 71e-4	1 8051	3 454e-3	0 4290
160×160	9 4e-5	1 5276	1 433e-3	1 2692
320×320	2 6e-5	1 8541	6 89e-4	1 0565
41×39	9 36e-4		5 356e-3	
81×79	2 58e-4	1 8591	3 144e-3	0 7686
161×159	7 7e-5	1 7444	1 390e-3	1 1775
321×319	2 2e-5	1 8074	6 47e-4	1 1032

$$\beta^-(x,y) = 2 + \sin(x+y), \tag{3 63}$$

$$u^+(x,y) = 8, \tag{3 64}$$

$$u^-(x,y) = (x^2+y^2)^{5/6} + \sin(x+y) \tag{3 65}$$

Figure 3 13 shows the computed solution with the current method using an 81×41 grid Table 3 7 shows the error on different grids

Example 6 This example has a "happy face" interface and matrix form $\beta^\pm$, with lower-order terms p, q present $\phi(x,y)$, $\beta^\pm(x,y)$ and $u^\pm(x,y)$ are

$$\phi(x,y) = \max(\min(\phi_1,\phi_2,\phi_3),\phi_4,\phi_5,\phi_6,\min(\phi_7,\phi_8)), \tag{3 66}$$

$$\phi_1(x,y) = x^2+y^2-0\ 75^2-0\ 15^2, \tag{3 67}$$

$$\phi_2(x,y) = (x-0\ 75)^2+y^2-0\ 15^2, \tag{3 68}$$

$$\phi_3(x,y) = (x+0\ 75)^2+y^2-0\ 15^2, \tag{3 69}$$

Table 3 6 Chess board Results using the method described in [15]

$n_x \times n_y$	Error in U	Order
40×40	2 38e-1	
80×80	7 88e-2	1 59
160×160	5 43e-2	0 54
320×320	2 57e-2	1 08
41×39	1 24e-1	
81×79	6 75e-2	0 88
161×159	4 56e-2	0 57
321×319	2 25e-2	1 02

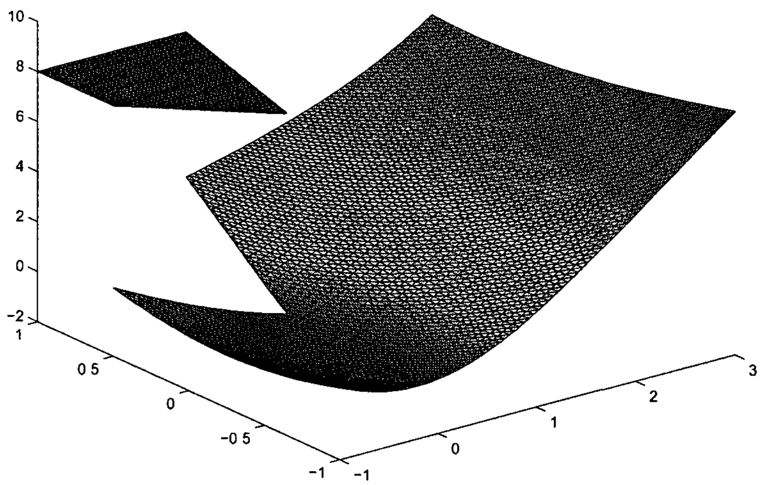

Figure 3 13 A singular point at $(0,0)$

$$\phi_4(x,y) = -\frac{0\ 1}{0\ 12}(x-0\ 2)^2 - \frac{0\ 12}{0\ 1}(y-0\ 22)^2 + 0\ 12\ \ 0\ 1, \quad (3\ 70)$$

$$\phi_5(x,y) = -\frac{0\ 1}{0\ 12}(x+0\ 2)^2 - \frac{0\ 12}{0\ 1}(y-0\ 22)^2 + 0\ 12\ \ 0\ 1, \quad (3\ 71)$$

Table 3 7 Singular point on the interface in two dimensions

$n_x \times n_y$	Error in U	Order	Error in ∇U	Order
41×21	4 940e-3		4 698e-2	
81×41	1 745e-3	1 5013	2 978e-2	0 6577
161×81	6 06e-4	1 5258	1 886e-2	0 6590
321×161	2 09e-4	1 5358	1 194e-2	0 6595

$$\phi_6(r,y) = -r^2 - (y+0\ 08)^2 + 0\ 12^2, \tag{3 72}$$

$$\phi_7(x,y) = -x^2 - (y+0\ 625)^2 + 0\ 425^2, \tag{3 73}$$

$$\phi_8(x,y) = -x^2 - (y+0\ 25)^2 + 0\ 2^2, \tag{3 74}$$

$$\beta^+(x,y) = \begin{pmatrix} (ry+2)/5 & 0 \\ 0 & (xy+2)/5 \end{pmatrix}, \tag{3 75}$$

$$\beta^-(x,y) = \begin{pmatrix} (x^2-y^2+3)/7 & 0 \\ 0 & (x^2-y^2+3)/7 \end{pmatrix}, \tag{3 76}$$

$$u^+(x,y) = 5 - 5x^2 - 5y^2, \tag{3 77}$$

$$u^-(x,y) = 7x^2 + 7y^2 + 1 \tag{3 78}$$

The computed solution with the current method using a 40×40 grid is shown in Figure 3 14 Table 3 8 shows the error on different grids using the current method Table 3 9 shows the error on different grids in [15] These two tables show that the accuracy is significantly improved The numerical result shows second-order accuracy in the L^∞ norm for the solution

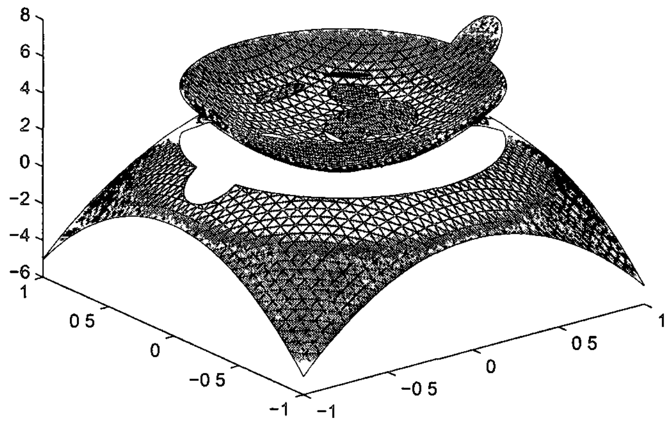

Figure 3 14 Happy face without lower-order terms

Table 3 8 Happy face without lower-order terms

$n_x \times n_y$	Error in U	Order
40×40	3 2575e-3	
80×80	8 1030e-4	2 0072
160×160	2 1751e-4	1 8974
320×320	6 4081e-5	1 7631

When the coefficients $\beta^{\pm}(x, y)$, $p^{\pm}(x, y)$ and $q^{\pm}(x, y)$ are

$$\beta^{+}(x, y) = \begin{pmatrix} xy+2 & xy+1 \\ xy+1 & xy+3 \end{pmatrix}, \tag{3 79}$$

$$\beta^{-}(x, y) = \begin{pmatrix} x^2-y^2+3 & x^2-y^2+1 \\ x^2-y^2+1 & x^2-y^2+4 \end{pmatrix}, \tag{3 80}$$

$$p^{+}(x, y) = \begin{pmatrix} xy \\ x^2-y^2-1 \end{pmatrix}, \tag{3 81}$$

Table 3 9 Happy face without lower-order terms in [15]

$n_x \times n_y$	Error in U	Order
40×40	6 06e-2	
80×80	1 64e-2	1 89
160×160	4 34e-3	1 92
320×320	1 15e-3	1 92

$$p^-(x,y) = \begin{pmatrix} x^2 - y^2 \\ 2xy - 1 \end{pmatrix}, \tag{3 82}$$

$$q^+(x,y) = x^2 + y^2 - 2, \tag{3 83}$$

$$q^-(x,y) = xy + 1 \tag{3 84}$$

The computed solution with the current method using a 40×40 grid is shown in Figure 3 15 Table 3 10 shows the error on different grids The numerical result shows second-order accuracy for the solution and first-order accuracy for the gradient in the L^∞ norm

From Table 3 5 and Table 3 7, the orders of the errors in u and ∇u are listed in Table 3 11

Compared with [15], when Γ is C^1, the current order of accuracy is consistent with [15], and when Γ is Lipschitz continuous, the current order of accuracy is higher than [15] Besides, for the same grid size, the current error is consistently smaller than [15], thanks to the more elegant quadrature formula discussed in Section 3 2

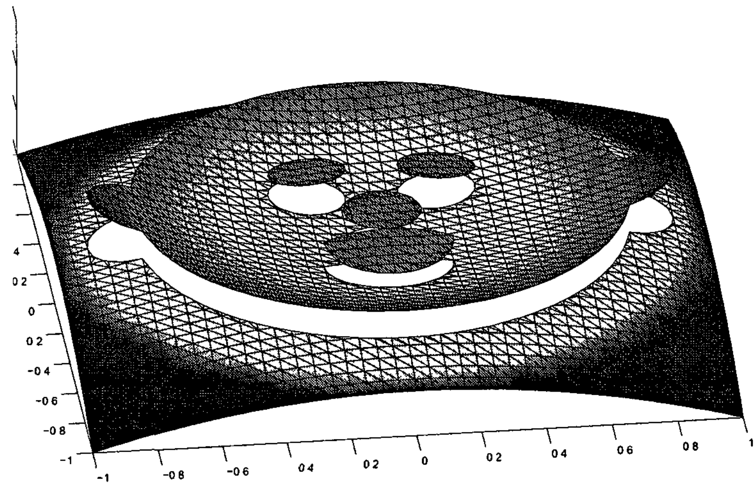

Figure 3 15 Happy face with lower-order terms

Table 3 10 Happy face with lower-order terms

$n_x \times n_y$	Error in U	Order	Error in ∇U	Order
40×40	5 931e-3		5 121e-2	
80×80	1 669e-3	1 8293	2 757e-2	0 8933
160×160	4 51e-4	1 8878	1 686e-2	0 7095
320×320	1 24e-4	1 8628	8 940e-3	0 9153

Table 3 11 Conclusion of numerical experiments

	Γ is C^1	Γ is Lipschitz continuous
u is C^2	2nd order in u, 1st order in ∇u	2nd order in u, 1st order in ∇u
u is C^1	1st order in u, 0 8th order in ∇u	1st order in u, 0 7th order in ∇u
u is H^2	1 6th order in u, 0 7th order in ∇u	1 5th order in u, 0 7th order in ∇u

CHAPTER 4

2-D ELASTICITY PROBLEM WITH TWO DOMAINS

In this chapter, based on the method in Chapter 3, a numerical method is proposed for solving the elasticity problem with sharp-edged interfaces It was proved that the resulting linear system is non-symmetric but positive definite under certain assumptions The method is simpler compared with that developed in [12] and can be applied for more general problems since the β_i are allowed to be matrices

4 1 The Weak Formulations

The variable coefficient elasticity interface problem is given by

$$\begin{cases} -\nabla \cdot (\beta_1(x)\nabla u_1(x)) - \nabla \cdot (\beta_2(x)\nabla u_2(x)) = f_1(x), \\ -\nabla \cdot (\beta_3(x)\nabla u_1(x)) - \nabla \cdot (\beta_4(x)\nabla u_2(x)) = f_2(x), \end{cases} \qquad x \in \Omega \setminus \Gamma, \tag{4 1}$$

where $x = (x_1, \ldots, x_d)$ is the spatial variables $\beta_i(x), i = 1, 2, 3, 4$ are assumed to be $d \times d$ matrices that are uniformly elliptic on Ω^- and Ω^+ $f_i(x), i = 1, 2$ is in $L^2(\Omega)$

The jump conditions are prescribed

$$\begin{cases} [u_1]_\Gamma(x) \equiv u_1^+(x) - u_1^-(x) = a_1(x), \\ [u_2]_\Gamma(x) \equiv u_2^+(x) - u_2^-(x) = a_2(x), \\ n \cdot (\beta_1^+(x)\nabla u_1^+(x) + \beta_2^+(x)\nabla u_2^+(x)) - \\ n \cdot (\beta_1^-(x)\nabla u_1^-(x) + \beta_2^-(x)\nabla u_2^-(x)) = b_1(x), \\ n \cdot (\beta_3^+(x)\nabla u_1^+(x) + \beta_4^+(x)\nabla u_2^+(x)) - \\ n \cdot (\beta_3^-(x)\nabla u_1^-(x) + \beta_4^-(x)\nabla u_2^-(x)) = b_2(x), \end{cases} \tag{4 2}$$

$a_{1,2}$ and $b_{1,2}$ are given functions along the interface Γ, "$\pm$" denote limits taken within $\Omega^\pm$

Functions $g_{1,2}$ are given on $\partial\Omega$, the boundary conditions are prescribed

$$\begin{cases} u_1(x) = g_1(x), \\ u_2(x) = g_2(x), \end{cases} \quad x \in \partial\Omega \tag{4 3}$$

The setup of the problem is illustrated in Figure 4 1

The weak formulation in [15, 16] is modified The usual Sobolev space $H^1(\Omega)$ is used For $H_0^1(\Omega)$, an inner product is chosen as

$$B[u,v] = \begin{cases} \int_{\Omega^+}(\beta_1\nabla u_1 \cdot \nabla v_1 + \beta_2\nabla u_2 \cdot \nabla v_1) + \int_{\Omega^-}(\beta_1\nabla u_1 \cdot \nabla v_1 + \beta_2\nabla u_2 \cdot \nabla v_1), \\ \int_{\Omega^+}(\beta_3\nabla u_1 \cdot \nabla v_2 + \beta_4\nabla u_2 \cdot \nabla v_2) + \int_{\Omega^-}(\beta_3\nabla u_1 \cdot \nabla v_2 + \beta_4\nabla u_2 \cdot \nabla v_2) \end{cases} \tag{4 4}$$

The weak formulation in [15, 16] is generalized for the elliptic equation with matrix coefficient

$$B[v,\psi] = \int_{\Omega^+} \beta\nabla v \cdot \nabla\psi + \int_{\Omega^-} \beta\nabla v \cdot \nabla\psi \tag{4 5}$$

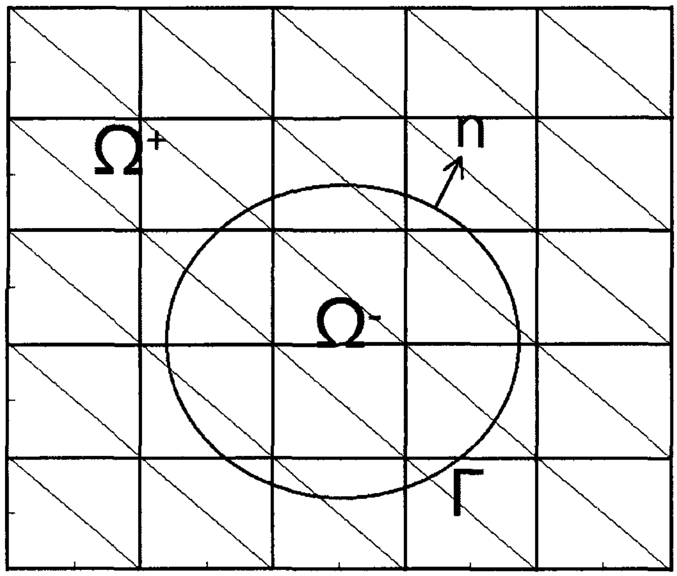

Figure 4 1 Setup of the problem with a uniform triangulation

Definition 4 1 1 $u \in H(a,c)$ is called a weak solution of Equations 4 1-4 3, if it satisfies, for all $\psi \in H_0^1(\Omega)$,

$$\begin{cases} \int_{\Omega^+}(\beta_1\nabla u_1 \cdot \nabla\psi_1 + \beta_2\nabla u_2 \cdot \nabla\psi_1) + \int_{\Omega^-}(\beta_1\nabla u_1 \cdot \nabla\psi_1 + \beta_2\nabla u_2 \cdot \nabla\psi_1) \\ = \int_\Omega f_1\psi_1 + \int_\Gamma b_1\psi_1, \\ \\ \int_{\Omega^+}(\beta_3\nabla u_1 \cdot \nabla\psi_2 + \beta_4\nabla u_2 \cdot \nabla\psi_2) + \int_{\Omega^-}(\beta_3\nabla u_1 \cdot \nabla\psi_2 + \beta_4\nabla u_2 \cdot \nabla\psi_2) \\ = \int_\Omega f_2\psi_2 + \int_\Gamma b_2\psi_2 \end{cases} \quad (4\ 6)$$

Theorem 4 1 2 If $f \in L^2(\Omega)$, a, b and $c \in H^1(\Omega)$, then there exists a unique weak solution of Equations 4 1-4 3 in $H(a,c)$

Proof See Theorem 2 1 in [15] □

4 2 Numerical Method

Define

$$u \equiv \begin{bmatrix} u_1 \\ u_2 \end{bmatrix}, \quad f \equiv \begin{bmatrix} f_1 \\ f_2 \end{bmatrix}, \quad g \equiv \begin{bmatrix} g_1 \\ g_2 \end{bmatrix},$$

$$a \equiv \begin{bmatrix} a_1 \\ a_2 \end{bmatrix}, \quad b \equiv \begin{bmatrix} b_1 \\ b_2 \end{bmatrix}, \quad \beta \equiv \begin{bmatrix} \beta_1 & \beta_2 \\ \beta_3 & \beta_4 \end{bmatrix}, \tag{4 7}$$

and choose a test function

$$\psi = \begin{bmatrix} \psi^1 \\ 0 \end{bmatrix} \text{ or } \begin{bmatrix} 0 \\ \psi^2 \end{bmatrix}, \tag{4 8}$$

and redefine the gradient and divergence operator

$$\nabla \equiv \begin{bmatrix} \frac{\partial}{\partial x} & 0 \\ \frac{\partial}{\partial y} & 0 \\ 0 & \frac{\partial}{\partial x} \\ 0 & \frac{\partial}{\partial y} \end{bmatrix}, \quad \nabla \cdot \equiv \begin{bmatrix} \frac{\partial}{\partial x} & \frac{\partial}{\partial y} & 0 & 0 \\ 0 & 0 & \frac{\partial}{\partial x} & \frac{\partial}{\partial y} \end{bmatrix} \tag{4 9}$$

Then Equation 4 1 can be written as

$$-\nabla \cdot (\beta(x)\nabla u(x)) = f(x), \quad x \in \Omega \setminus \Gamma, \tag{4 10}$$

the jump condition Equation 4 2 can be reformulated as

$$\begin{cases} [u]_\Gamma(x) \equiv u^+(x) - u^-(x) = a(x), \\ n \cdot (\beta^+(x)\nabla u^+(x)) - n \cdot (\beta^-(x)\nabla u^-(x)) = b(x), \end{cases} \tag{4 11}$$

and the boundary condition is

$$u(x) = g(x) \quad x \in \partial\Omega \tag{4 12}$$

For simplicity, the following properties are discussed under the form of Equations 4 10, 4 11, and 4 12

A cell $\triangle_k$ with corners k_1, k_2, k_3 belongs to one of two different sets

$$\begin{aligned}
\Lambda_1 &= \{\triangle_k \subset \Omega \quad k_1, k_2, k_3 \text{ are in the same domain among } \Omega^{\pm}\}, \\
\Lambda_2 &= \{\triangle_k \subset \Omega \quad k_1, k_2, k_3 \text{ are in two different domains among } \Omega^{\pm}\}
\end{aligned}$$

If a cell belongs to Λ_1, it is a regular cell, otherwise it is an interface cell An interface cell is separated by a straight line segment, denoted by Γ_K^h

Theorem 4 2 1 If β is positive definite, then the matrix A for the linear system generated by the current method is positive definite

Proof See proof of Theorem 3 2 4 in Chapter 3 □

In some applications in [12], the matrix β is only semi-positive definite with zero determinant The above theorem does not apply Below is the proof that when the matrix β is of a certain form frequently appearing in applications and semi-positive definite, then the matrix A generated by the current method is still positive definite

Theorem 4 2 2 If $\lambda > 0,\ \mu > 0$ and $\beta_1 = \begin{bmatrix} \lambda + 2\mu & 0 \\ 0 & \mu \end{bmatrix}$, $\beta_2 = \begin{bmatrix} 0 & \lambda \\ \mu & 0 \end{bmatrix}$, $\beta_3 = \begin{bmatrix} 0 & \mu \\ \lambda & 0 \end{bmatrix}$, $\beta_4 = \begin{bmatrix} \mu & 0 \\ 0 & \lambda + 2\mu \end{bmatrix}$, then the matrix A for the linear system generated by the current method is positive definite

Proof Suppose for a contradiction that A is not positive definite Then there is a vector $c \in R^{2n}$ and $c \neq 0$ such that $c^T A c \leq 0$ Let

$$w = \begin{bmatrix} w_1 \\ w_2 \end{bmatrix} = \sum_{i=1}^{2n} c_i \psi_i = \sum_{i=1}^{2n} c_i u_i,$$

then

$$
\begin{aligned}
& B[w,w] \le 0, \\
\Rightarrow \quad & \int_\Omega (\beta \nabla w(\vec{x}))^T \nabla w(x) \mathrm{d}\vec{x} \le 0, \\
\Rightarrow \quad & \int_\Omega \begin{bmatrix} \frac{\partial w_1}{\partial x} & \frac{\partial w_1}{\partial y} & \frac{\partial w_2}{\partial x} & \frac{\partial w_2}{\partial y} \end{bmatrix} \begin{bmatrix} \lambda+2\mu & 0 & 0 & \lambda \\ 0 & \mu & \mu & 0 \\ 0 & \mu & \mu & 0 \\ \lambda & 0 & 0 & \lambda+2\mu \end{bmatrix} \begin{bmatrix} \frac{\partial w_1}{\partial x} \\ \frac{\partial w_1}{\partial y} \\ \frac{\partial w_2}{\partial x} \\ \frac{\partial w_2}{\partial y} \end{bmatrix} \mathrm{d}\vec{x} \le 0
\end{aligned}
\tag{4 13}
$$

Since for all $a = [a_1, a_2, a_3, a_4]^T \in R^4$,

$$
a^T \beta a = (a_1 + a_4)^2 \lambda + 2(a_1^2 + a_4^2)\mu + (a_2 + a_3)^2 \mu \ge 0 \tag{4 14}
$$

So $a^T\beta a = 0$ if and only if $a_1 = a_4 = 0$ and $a_2 = -a_3$ Then $\frac{\partial w_1}{\partial x}(\vec{x}) = a_1 = 0,\ \forall \vec{x} \in \Omega$ However, $w_1 = \sum_{i=1}^n c_i \psi_i^1$ implies $\frac{\partial w_1}{\partial x} = \sum_{i=1}^n c_i \frac{\partial \psi_i^1}{\partial x}$ Since $c = [c_1, c_2, \quad , c_{2n}]^T \neq 0$, without loss of generality, it is assumed that $c_1 \neq 0$ If a point $\vec{x} \in \Omega$ is chosen such that $\frac{\partial \psi_1^1(\vec{x})}{\partial x} \neq 0$ and $\frac{\partial \psi_i^1(\vec{x})}{\partial x} = 0,\ i = 2, 3, \quad , n$, then $\sum_{i=1}^n c_i \frac{\partial \psi_i^1}{\partial x} \neq 0$, a contradiction Therefore $c^T A c > 0\ \forall c \neq 0$, that is, A is positive definite $\square$

From Remark 2 in Chapter 3, it is known that a positive definite matrix has positive determinant, and is therefore invertible The linear system $Ax = b$ can be solved efficiently

4.3 Numerical Experiments

Consider the problem

$$\begin{cases} -\nabla\cdot(\beta_1\nabla u_1)-\nabla\cdot(\beta_2\nabla u_2)=f_1, \text{ in } \Omega^{\pm}, \\ \\ -\nabla\cdot(\beta_3\nabla u_1)-\nabla\cdot(\beta_4\nabla u_2)=f_2, \text{ in } \Omega^{\pm}. \end{cases} \tag{4.15}$$

The jump conditions and boundary conditions are given as

$$\begin{cases} [u_1]=a_1, \text{ on } \Gamma, \\ \\ [u_2]=a_2, \text{ on } \Gamma, \\ \\ [(\beta_1\nabla u_1+\beta_2\nabla u_2)\cdot n]=b_1, \text{ on } \Gamma, \\ \\ [(\beta_3\nabla u_1+\beta_4\nabla u_2)\cdot n]=b_2, \text{ on } \Gamma, \\ \\ u_1=g_1, \text{ on } \partial\Omega, \\ \\ u_2=g_2, \text{ on } \partial\Omega, \end{cases} \tag{4.16}$$

on the rectangular domain $\Omega=(x_{min},x_{max})\times(y_{min},y_{max})$. The interface Γ is prescribed by a level-set function $\phi(x,y)$. $n=\frac{\nabla\phi}{|\nabla\phi|}$ is the unit normal vector pointing from Ω^- to Ω^+.

In all examples of this section, given $\phi(x,y)$, $\beta_{1,2,3,4}(x,y)$ and

$$\begin{cases} u_1=u_1^+(x,y), \text{ in } \Omega^+, \\ u_2=u_2^+(x,y), \text{ in } \Omega^+, \\ u_1=u_1^-(x,y), \text{ in } \Omega^-, \\ u_2=u_2^-(x,y), \text{ in } \Omega^-. \end{cases} \tag{4.17}$$

Hence, on Ω,

$$\begin{cases} f_1 = -\nabla \cdot (\beta_1 \nabla u_1) - \nabla \cdot (\beta_2 \nabla u_2), \\ f_2 = -\nabla \cdot (\beta_3 \nabla u_1) - \nabla \cdot (\beta_4 \nabla u_2), \\ a_1 = u_1^+ - u_1^-, \\ a_2 = u_2^+ - u_2^-, \\ b_1 = (\beta_1^+ \nabla u_1^+ + \beta_2^+ \nabla u_2^+) \cdot n - (\beta_1^- \nabla u_1^- + \beta_2^- \nabla u_2^-) \cdot n, \\ b_2 = (\beta_3^+ \nabla u_1^+ + \beta_4^+ \nabla u_2^+) \cdot n - (\beta_3^- \nabla u_1^- + \beta_4^- \nabla u_2^-) \cdot n, \end{cases} \tag{4.18}$$

g is obtained from the given solutions as a proper Dirichlet boundary condition

All errors of solutions are measured in the L^∞ norm in the whole domain Ω

Four numerical examples are presented in this chapter to demonstrate the effectiveness of the method

Example 7 This example has a smooth interface $\phi(x,y)$, $\beta_1^\pm(x,y)$, $\beta_2^\pm(x,y)$, $\beta_3^\pm(x,y)$, $\beta_4^\pm(x,y)$ and $u_1^\pm(x,y)$, $u_2^\pm(x,y)$ are

$$\phi(x,y) = x^2 + y^2 - 0.25, \tag{4.19}$$

$$\beta_1^+(x,y) = \begin{pmatrix} x^2+3 & \sin(x+y)+1 \\ 0.5\sin(x+y)+0.7 & y^2+5 \end{pmatrix}, \tag{4.20}$$

$$\beta_1^-(x,y) = \begin{pmatrix} x^2+y^2+3 & \sin(xy)+1 \\ \sin(x+y)+1 & y^2+4 \end{pmatrix}, \tag{4.21}$$

$$\beta_2^+(x,y) = \begin{pmatrix} \cos(x)^2+0.1 & (x+y)^2+2 \\ 2x^2 & 0.6\cos(x)+1 \end{pmatrix}, \tag{4.22}$$

$$\beta_2^-(x,y) = \begin{pmatrix} \cos(y)+1 & (x+y)^2+1 \\ 2x^2+1 & 0.5\cos(x)^2 \end{pmatrix}, \tag{4.23}$$

$$\beta_3^+(x,y) = \begin{pmatrix} \cos(x+y)^2 & 3x^2y^2 \\ x^2+1 & \cos(y)+1 \end{pmatrix}, \tag{4 24}$$

$$\beta_3^-(x,y) = \begin{pmatrix} 2\cos(x+y)^2 & 3x^2y^2+0\ 1 \\ 2x^2 & 2\cos(xy)+2 \end{pmatrix}, \tag{4 25}$$

$$\beta_4^+(x,y) = \begin{pmatrix} x^2y^2+5 & (\sin(x+2y))^2 \\ \sin(x+2y)+1 & y^2+x^2+3 \end{pmatrix}, \tag{4 26}$$

$$\beta_4^-(x,y) = \begin{pmatrix} 0\ 5x^2y^2+4 & \sin(x)+1 \\ \sin(x+y)+1 & y^2+x^2+4 \end{pmatrix}, \tag{4 27}$$

$$u_1^+(x,y) = x^2+y^2-\sin(x+y), \tag{4 28}$$

$$u_1^-(x,y) = (\sqrt{(x^2+y^2)})^2, \tag{4 29}$$

$$u_2^+(x,y) = 2y(x^3)+y^2, \tag{4 30}$$

$$u_2^-(x,y) = (\sqrt{(x^2+y^2)})^3 \tag{4 31}$$

The computed solutions with the current method using a 48 × 48 grid are shown in Figures 4 2 and 4 3 Table 4 1 shows the error on different grids The numerical result shows second-order accuracy in the L^∞ norm for the solution

Example 8 This example is a "happy face" interface with corners $\phi(x,y)$, $\beta_1^\pm(x,y)$, $\beta_2^\pm(x,y)$, $\beta_3^\pm(x,y)$, $\beta_4^\pm(x,y)$ and $u_1^\pm(x,y)$, $u_2^\pm(x,y)$ are

$$\phi(x,y) = \max(\min(\phi_1,\phi_2,\phi_3),\phi_4,\phi_5,\phi_6,\min(\phi_7,\phi_8)), \tag{4 32}$$

$$\phi_1(x,y) = x^2+y^2-0\ 75^2-0\ 15^2, \tag{4 33}$$

$$\phi_2(x,y) = (x-0\ 75)^2+y^2-0\ 15^2, \tag{4 34}$$

$$\phi_3(x,y) = (x+0\ 75)^2+y^2-0\ 15^2, \tag{4 35}$$

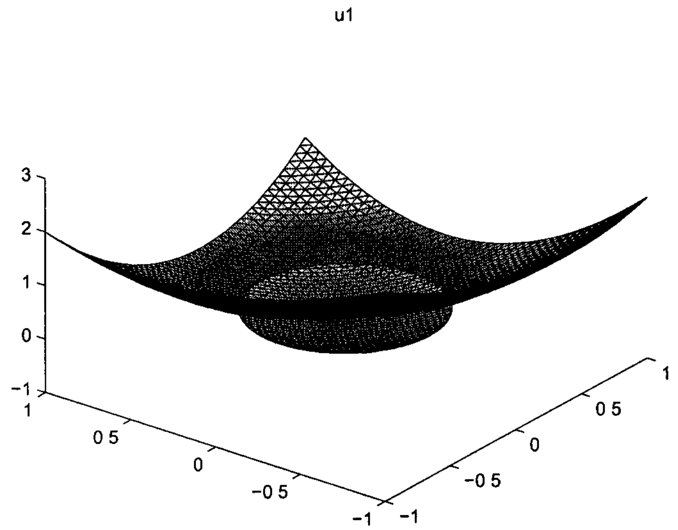

Figure 4 2 The solution u_1 with a smooth circular interface

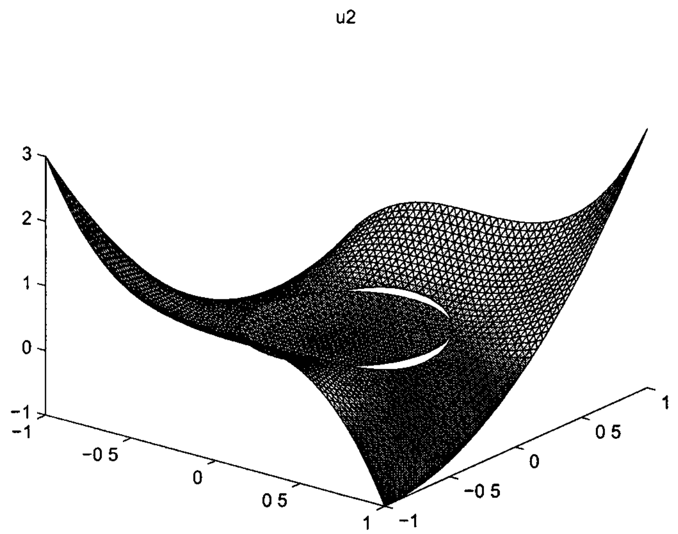

Figure 4 3 The solution u_2 with a smooth circular interface

$$\phi_4(x,y) = -\frac{0\ 1}{0\ 12}(x-0\ 2)^2 - \frac{0\ 12}{0\ 1}(y-0\ 22)^2 + 0\ 12\quad 0\ 1, \tag{4 36}$$

$$\phi_5(x,y) = -\frac{0\ 1}{0\ 12}(x+0\ 2)^2 - \frac{0\ 12}{0\ 1}(y-0\ 22)^2 + 0\ 12\quad 0\ 1, \tag{4 37}$$

$$\phi_6(x,y) = -x^2 - (y+0\ 08)^2 + 0\ 12^2, \tag{4 38}$$

$$\phi_7(x,y) = -x^2 - (y+0\ 625)^2 + 0\ 425^2, \tag{4 39}$$

Table 4 1 Circle shape interface

$n_x \times n_y$	Error in U	Order
24×24	0 00558	
48×48	0 00147	1 92
96×96	3 76e-004	1 97
192×192	9 48e-005	1 99
384×384	2 39e-005	1 99

$$\phi_8(x,y) = -x^2 - (y + 0\ 25)^2 + 0\ 2^2, \tag{4 40}$$

$$\beta_1^+(x,y) = \begin{pmatrix} x^2+3 & \sin(x+y)+1 \\ 0\ 5\sin(x+y)+0\ 7 & y^2+5 \end{pmatrix}, \tag{4 41}$$

$$\beta_1^-(x,y) = \begin{pmatrix} x^2+y^2+3 & \sin(xy)+1 \\ \sin(x+y)+1 & y^2+4 \end{pmatrix}, \tag{4 42}$$

$$\beta_2^+(r,y) = \begin{pmatrix} \cos(x)^2+0\ 1 & (x+y)^2+2 \\ 2x^2 & 0\ 6\cos(x)+1 \end{pmatrix}, \tag{4 43}$$

$$\beta_2^-(x,y) = \begin{pmatrix} \cos(y)+1 & (x+y)^2+1 \\ 2x^2+1 & 0\ 5\cos(x)^2 \end{pmatrix}, \tag{4 44}$$

$$\beta_3^+(x,y) = \begin{pmatrix} \cos(x+y)^2 & 3x^2y^2 \\ x^2+1 & \cos(y)+1 \end{pmatrix}, \tag{4 45}$$

$$\beta_3^-(x,y) = \begin{pmatrix} 2\cos(x+y)^2 & 3x^2y^2+0\ 1 \\ 2x^2 & 2\cos(xy)+2 \end{pmatrix}, \tag{4 46}$$

$$\beta_4^+(x,y) = \begin{pmatrix} x^2y^2+5 & (\sin(x+2y))^2 \\ \sin(x+2y)+1 & y^2+x^2+3 \end{pmatrix}, \tag{4 47}$$

$$\beta_4^-(x,y) = \begin{pmatrix} 0\,5x^2y^2+4 & \sin(x)+1 \\ \sin(x+y)+1 & y^2+x^2+4 \end{pmatrix}, \tag{4 48}$$

$$u_1^+(x,y) = x^2+y^2-\sin(x+y), \tag{4 49}$$

$$u_1^-(x,y) = (\sqrt{(x^2+y^2)})^2, \tag{4 50}$$

$$u_2^+(x,y) = 2y(x^3)+y^2, \tag{4 51}$$

$$u_2^-(x,y) = (\sqrt{(x^2+y^2)})^3 \tag{4 52}$$

The computed solutions with the current method using a 48×48 grid are shown in Figures 4 4 and 4 5 Table 4 2 shows the error on different grids The numerical result shows second-order accuracy in the L^∞ norm for the solution and first-order accuracy in the L^∞ norm for the gradient

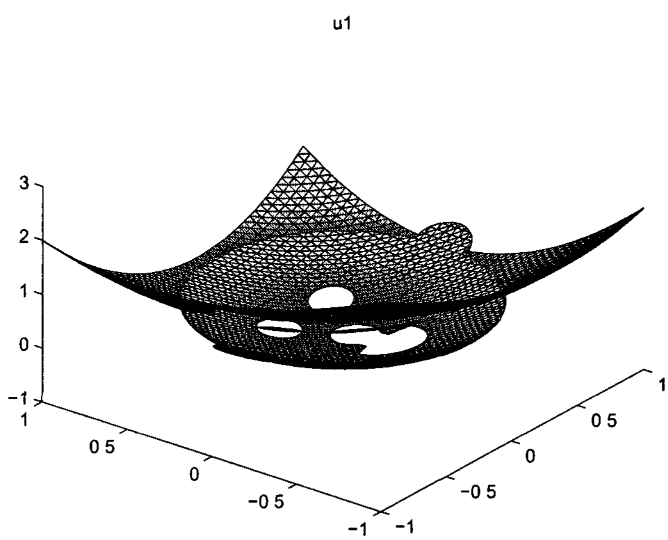

Figure 4 4 The solution u_1 with a "Happy face" interface

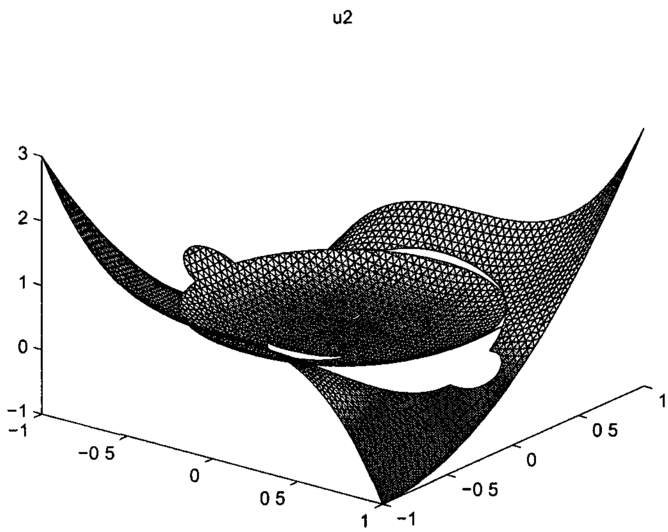

Figure 4 5 The solution u_2 with a "Happy face" interface

Table 4 2 Face shape interface

$n_x \times n_y$	Error in U	Order
24×24	0 00663	
48×48	0 00178	1 89
96×96	4 71e-004	1 92
192×192	1 21e-004	1 96
384×384	3 16e-005	1 94

Example 9 This example is a "star" interface $\phi(x,y)$, $\beta_1^{\pm}(x,y)$, $\beta_2^{\pm}(x,y)$, $\beta_3^{\pm}(x,y)$, $\beta_4^{\pm}(x,y)$ and $u_1^{\pm}(x,y)$, $u_2^{\pm}(x,y)$ are

$$\begin{aligned}
\phi(r,\theta) &= \frac{R\sin(\theta_t/2)}{\sin(\theta_t/2+\theta-\theta_r-2\pi(i-1)/5)} - r \\
&\quad \theta_r + \pi(2i-2)/5 \le \theta < \theta_r + \pi(2i-1)/5, \qquad (4\ 53) \\
\phi(r,\theta) &= \frac{R\sin(\theta_t/2)}{\sin(\theta_t/2-\theta+\theta_r-2\pi(i-1)/5)} - r
\end{aligned}$$

$$\theta_r + \pi(2i-3)/5 \leq \theta < \theta_r + \pi(2i-2)/5, \tag{4.54}$$

with $\theta_t = \pi/5,\ \theta_r = \pi/7,\ R = 6/7$ and $i = 1,2,3,4,5,$

$$\beta_1^+(x,y) = \begin{pmatrix} x^2+3 & \sin(x+y)+1 \\ 0.5\sin(x+y)+0.7 & y^2+5 \end{pmatrix}, \tag{4.55}$$

$$\beta_1^-(x,y) = \begin{pmatrix} x^2+y^2+3 & \sin(xy)+1 \\ \sin(x+y)+1 & y^2+4 \end{pmatrix}, \tag{4.56}$$

$$\beta_2^+(x,y) = \begin{pmatrix} \cos(x)^2+0.1 & (x+y)^2+2 \\ 2x^2 & 0.6\cos(x)+1 \end{pmatrix}, \tag{4.57}$$

$$\beta_2^-(x,y) = \begin{pmatrix} \cos(y)+1 & (x+y)^2+1 \\ 2x^2+1 & 0.5\cos(x)^2 \end{pmatrix}, \tag{4.58}$$

$$\beta_3^+(x,y) = \begin{pmatrix} \cos(x+y)^2 & 3x^2y^2 \\ x^2+1 & \cos(y)+1 \end{pmatrix}, \tag{4.59}$$

$$\beta_3^-(x,y) = \begin{pmatrix} 2\cos(x+y)^2 & 3x^2y^2+0.1 \\ 2x^2 & 2\cos(xy)+2 \end{pmatrix}, \tag{4.60}$$

$$\beta_4^+(x,y) = \begin{pmatrix} x^2y^2+5 & (\sin(x+2y))^2 \\ \sin(x+2y)+1 & y^2+x^2+3 \end{pmatrix}, \tag{4.61}$$

$$\beta_4^-(x,y) = \begin{pmatrix} 0.5x^2y^2+4 & \sin(x)+1 \\ \sin(x+y)+1 & y^2+x^2+4 \end{pmatrix}, \tag{4.62}$$

$$u_1^+(x,y) = x^2+y^2-\sin(x+y), \tag{4.63}$$

$$u_1^-(x,y) = (\sqrt{(x^2+y^2)})^2, \tag{4.64}$$

$$u_2^+(x,y) = 2y(x^3)+y^2, \tag{4.65}$$

$$u_2^-(x,y) = (\sqrt{(x^2+y^2)})^3 \tag{4 66}$$

The computed solutions with the current method using a 48×48 grid are shown in Figures 4 6 and 4 7 Table 4 3 shows the error on different grids The numerical result shows second-order accuracy in the L^∞ norm for the solution and first-order accuracy in the L^∞ norm for the gradient

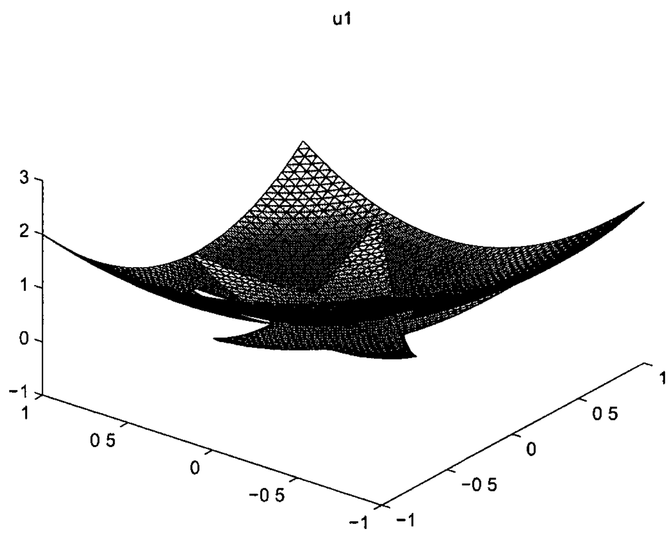

Figure 4 6 The solution u_1 with a "Star" interface

Example 10 The solutions in this example have a singularity on the interface corner $\phi(x,y)$, $\beta_1^\pm(x,y)$, $\beta_2^\pm(x,y)$, $\beta_3^\pm(x,y)$, $\beta_4^\pm(x,y)$ and $u_1^\pm(x,y)$, $u_2^\pm(x,y)$ are

$$\phi(x,y) = (x-0\ 4)^2 + y^2 - 0\ 16, \tag{4 67}$$

$$\beta_1^+(x,y) = \begin{pmatrix} x^2+3 & \sin(x+y)+1 \\ 0\ 5\sin(x+y)+0\ 7 & y^2+5 \end{pmatrix}, \tag{4 68}$$

$$\beta_1^-(x,y) = \begin{pmatrix} x^2+y^2+3 & \sin(xy)+1 \\ \sin(x+y)+1 & y^2+4 \end{pmatrix}, \tag{4 69}$$

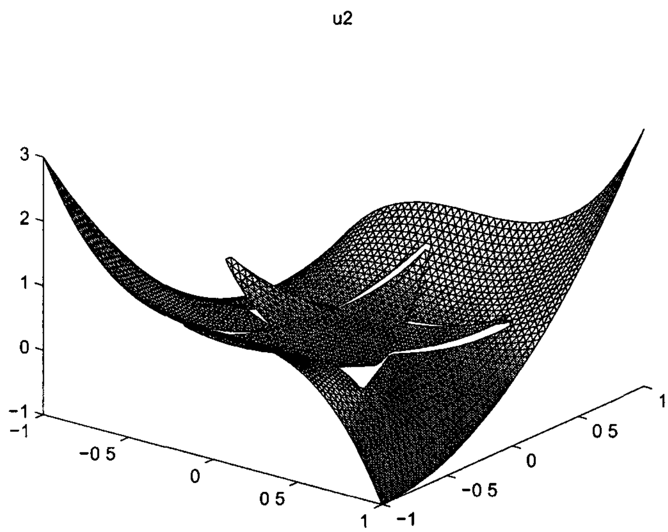

Figure 4 7 The solution u_2 with a "Star" interface

Table 4 3 Star shape interface

$n_x \times n_y$	Error in U	Order
24×24	0 00533	
48×48	0 00159	1 75
96×96	4 22e-004	1 91
192×192	1 10e-004	1 94
384×384	2 90e-005	1 93

$$\beta_2^+(x,y) = \begin{pmatrix} \cos(x)^2 + 0\,1 & (x+y)^2 + 2 \\ 2x^2 & 0\,6\cos(x) + 1 \end{pmatrix}, \tag{4 70}$$

$$\beta_2^-(x,y) = \begin{pmatrix} \cos(y) + 1 & (x+y)^2 + 1 \\ 2x^2 + 1 & 0\,5\cos(x)^2 \end{pmatrix}, \tag{4 71}$$

$$\beta_3^+(x,y) = \begin{pmatrix} \cos(x+y)^2 & 3x^2y^2 \\ x^2+1 & \cos(y)+1 \end{pmatrix}, \tag{4 72}$$

$$\beta_3^-(x,y) = \begin{pmatrix} 2\cos(x+y)^2 & 3x^2y^2+0\ 1 \\ 2x^2 & 2\cos(xy)+2 \end{pmatrix}, \tag{4 73}$$

$$\beta_4^+(x,y) = \begin{pmatrix} x^2y^2+5 & (\sin(x+2y))^2 \\ \sin(x+2y)+1 & y^2+x^2+3 \end{pmatrix}, \tag{4 74}$$

$$\beta_4^-(x,y) = \begin{pmatrix} 0\ 5x^2y^2+4 & \sin(x)+1 \\ \sin(x+y)+1 & y^2+x^2+4 \end{pmatrix}, \tag{4 75}$$

$$u_1^+(x,y) = (x^2+y^2)^{5/6}, \tag{4 76}$$

$$u_1^-(x,y) = 1, \tag{4 77}$$

$$u_2^+(x,y) = x, \tag{4 78}$$

$$u_2^-(x,y) = 0 \tag{4 79}$$

The computed solutions with the current method using a 48×48 grid are shown in Figures 4 8 and 4 9 Table 4 4 shows the error on different grids

Example 11 This example has the special type of coefficients that satisfies the hypothesis of Theorem 3 2 $\phi(x,y)$, $\beta_1^\pm(x,y)$, $\beta_2^\pm(x,y)$, $\beta_3^\pm(x,y)$, $\beta_4^\pm(x,y)$ and $u_1^\pm(x,y)$, $u_2^\pm(x,y)$ are

$$\phi(r,y) = r^2+y^2-0\ 16, \tag{4 80}$$

$$\beta_1^+(x,y) = \begin{pmatrix} 8 & 0 \\ 0 & 4 \end{pmatrix}, \tag{4 81}$$

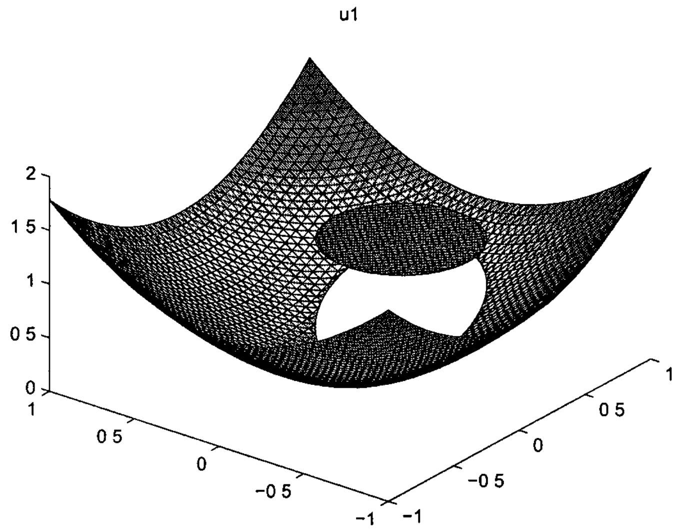

Figure 4 8 The solution u_1 with a singular point on the interface

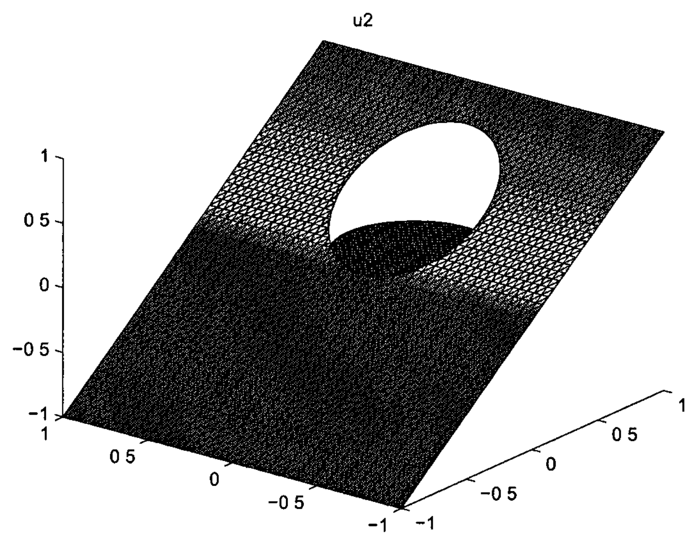

Figure 4 9 The solution u_2 with a singular point on the interface

$$\beta_1^-(x,y) = \begin{pmatrix} 7 & 0 \\ 0 & 2 \end{pmatrix}, \tag{4 82}$$

$$\beta_2^+(x,y) = \begin{pmatrix} 0 & 2 \\ 4 & 0 \end{pmatrix}, \tag{4 83}$$

Table 4 4 Singular point on the interface

$n_x \times n_y$	Error in U	Order
24×24	0 00347	
48×48	0 00118	1 55
96×96	4 05e-004	1 55
192×192	1 39e-004	1 54
384×384	4 78e-005	1 54

$$\beta_2^-(x,y) = \begin{pmatrix} 0 & 3 \\ 2 & 0 \end{pmatrix}, \tag{4 84}$$

$$\beta_3^+(x,y) = \begin{pmatrix} 0 & 4 \\ 2 & 0 \end{pmatrix}, \tag{4 85}$$

$$\beta_3^-(x,y) = \begin{pmatrix} 0 & 2 \\ 3 & 0 \end{pmatrix}, \tag{4 86}$$

$$\beta_4^+(r,y) = \begin{pmatrix} 4 & 0 \\ 0 & 8 \end{pmatrix}, \tag{4 87}$$

$$\beta_4^-(x,y) = \begin{pmatrix} 2 & 0 \\ 0 & 7 \end{pmatrix}, \tag{4 88}$$

$$u_1^+(x,y) = \sin(x)\cos(y), \tag{4 89}$$

$$u_1^-(x,y) = x\sin(y), \tag{4 90}$$

$$u_2^+(x,y) = \cos(x) + y^2, \tag{4 91}$$

$$u_2^-(x,y) = xy \tag{4 92}$$

The computed solutions with the current method using a 48×48 grid are shown in Figures 4 10 and 4 11 Table 4 5 shows the error on different grids

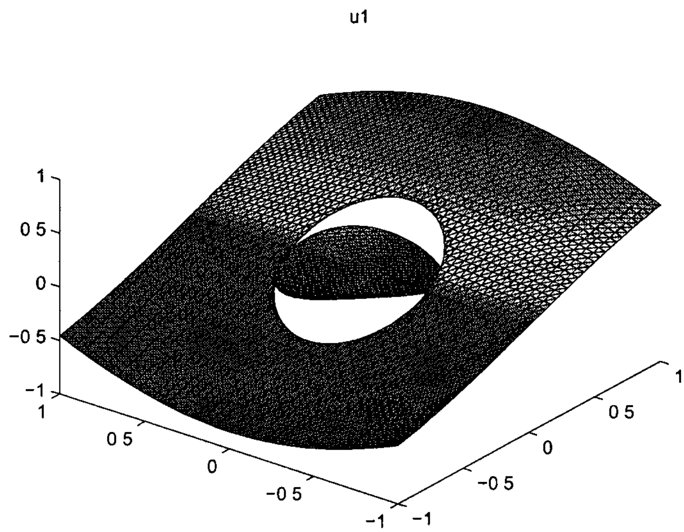

Figure 4 10 The solution u_1 with coefficients of special form

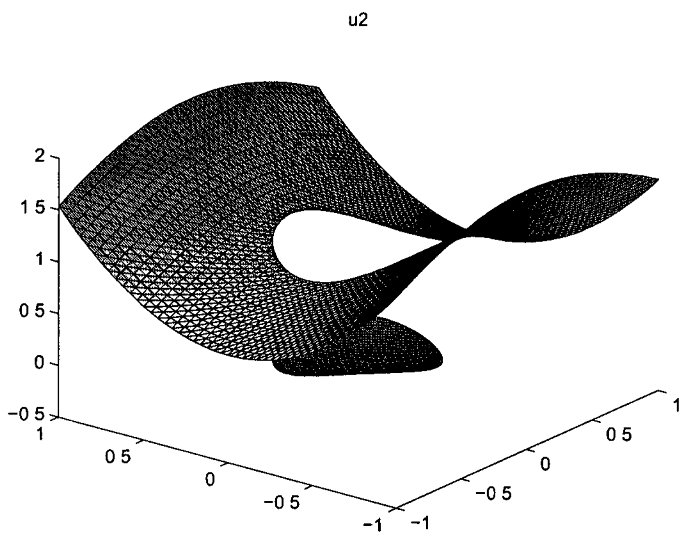

Figure 4 11 The solution u_2 with coefficients of special form

Table 4 5 Specıal form of coefficıents

$n_x \times n_y$	Error ın U	Order
24×24	0 00151	
48×48	4 44e-004	1 77
96×96	1 20e-004	1 89
192×192	3 30e-005	1 86
384×384	8 66e-006	1 93

CHAPTER 5

2-D ELLIPTIC PROBLEM WITH THREE DOMAINS

Based on the method in Chapter 3, this chapter proposes a numerical method for solving the elliptic problem with three domains An accurate treatment for the triple junction point shown in Figure 5 2 is proposed It has been proved that the resulting linear system is non-symmetric but positive definite if β_i, $i = 1, 2, 3$ are positive definite for the three domains Numerical results demonstrate near second-order accuracy for the method for piecewise smooth solutions

5 1 Equations and Weak Formulations

Let $\Omega \subset R^d$ be an open bounded domain, and let Γ be an interface Γ divides Ω into Ω_1, Ω_2 and Ω_3, hence $\Omega = \Omega_1 \bigcup \Omega_2 \bigcup \Omega_3 \bigcup \Gamma$, see Figure 5 1 Assuming that $\partial\Omega$ and $\partial\Omega_{1,2,3}$ are Lipschitz continuous as submanifolds, so is Γ A unit normal vector of Γ can be defined almost everywhere on Γ (see Section 1 5 in [13])

The variable coefficient elliptic interface problem is given by

$$-\nabla \cdot (\beta(x) \nabla u(x)) = f(x), \quad x \in \Omega \setminus \Gamma, \tag{5 1}$$

where $x = (x_1, \ldots, x_d)$ is the spatial variable $\beta(x)$ is a $d \times d$ matrix that is uniformly elliptic on each disjoint subdomain, Ω_1, Ω_2 and Ω_3 $f(x)$ is in $L^2(\Omega)$

Consider the problem on the rectangular domain $\Omega = (x_{min}, x_{max}) \times (y_{min}, y_{max}) = \Omega_1 \bigcup \Omega_2 \bigcup \Omega_3 \quad \Gamma_j, \; j = 1, 2, 3$

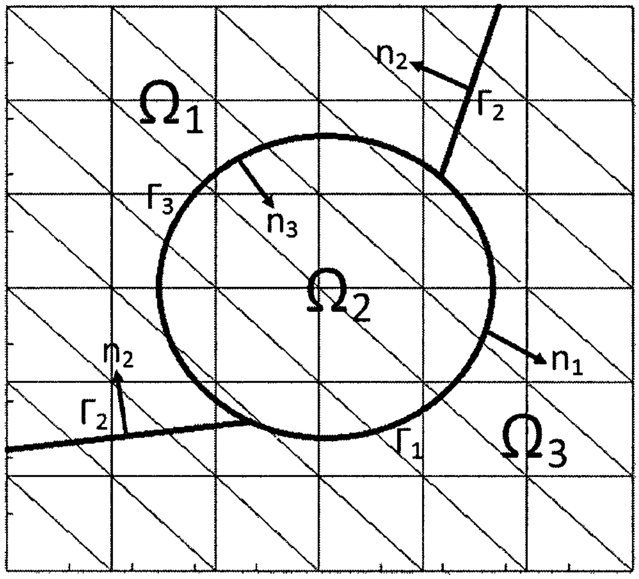

Figure 5 1 A uniform triangulation

$$
\begin{cases}
-\nabla \cdot (\beta_1 \nabla u_1) = f_1, \text{ in } \Omega_1, \\
-\nabla \cdot (\beta_2 \nabla u_2) = f_2, \text{ in } \Omega_2, \\
-\nabla \cdot (\beta_3 \nabla u_3) = f_3, \text{ in } \Omega_3
\end{cases}
\tag{5 2}
$$

The jump conditions are prescribed as

$$
\begin{cases}
[u]_{\Gamma_1} = u_2 - u_3 = a_1, \text{ on } \Gamma_1, \\
[u]_{\Gamma_2} = u_3 - u_1 = a_2, \text{ on } \Gamma_2, \\
[u]_{\Gamma_3} = u_1 - u_2 = a_3, \text{ on } \Gamma_3, \\
[\beta \nabla u]_{\Gamma_1} = (\beta_2 \nabla u_2 - \beta_3 \nabla u_3) \cdot n_1 = b_1, \text{ on } \Gamma_1, \\
[\beta \nabla u]_{\Gamma_2} = (\beta_3 \nabla u_3 - \beta_1 \nabla u_1) \cdot n_2 = b_2, \text{ on } \Gamma_2, \\
[\beta \nabla u]_{\Gamma_3} = (\beta_1 \nabla u_1 - \beta_2 \nabla u_2) \cdot n_3 = b_3, \text{ on } \Gamma_3
\end{cases}
\tag{5 3}
$$

a and b are given functions along the interfaces $\Gamma = \Gamma_1 \bigcup \Gamma_2 \bigcup \Gamma_3$, the "1, 2, 3" subscripts denote limits taken within $\Omega_{1,2,3}$

The boundary conditions are prescribed as

$$\begin{cases} u_1 = g_1, \text{ on } \partial\Omega \bigcap \partial\Omega_1, \\ u_2 = g_2, \text{ on } \partial\Omega \bigcap \partial\Omega_2, \\ u_3 = g_3, \text{ on } \partial\Omega \bigcap \partial\Omega_3 \end{cases} \tag{5.4}$$

The interfaces are prescribed by level-set functions $\phi_j(x, y)$

$$\phi_1(x,y) \begin{cases} < 0, \ (x,y) \in \Omega_3, \\ = 0, \ (x,y) \in \Gamma_1, \\ > 0, \ (x,y) \in \Omega_2 \end{cases} \tag{5.5}$$

$$\phi_2(x,y) \begin{cases} < 0, \ (x,y) \in \Omega_1, \\ = 0, \ (x,y) \in \Gamma_2, \\ > 0, \ (x,y) \in \Omega_3 \end{cases} \tag{5.6}$$

$$\phi_3(x,y) \begin{cases} < 0, \ (x,y) \in \Omega_2, \\ = 0, \ (x,y) \in \Gamma_3, \\ > 0, \ (x,y) \in \Omega_1 \end{cases} \tag{5.7}$$

The unit normal vector of Γ_j is $n_j = \frac{\nabla \phi_j}{|\nabla \phi_j|}$ pointing from $\Omega_j^- = \{(x,y) \in \Omega \mid \phi_j(x,y) \leq 0\}$ to $\Omega_j^+ = \{(x,y) \in \Omega \mid \phi_j(x,y) \geq 0\}$ for $j = 1, 2, 3$.

The weak formulation is generalized in [15, 16] for the elliptic equation with matrix coefficients. The usual Sobolev space $H^1(\Omega)$ is used. For $H_0^1(\Omega)$, an inner product is chosen as

$$B[u,v] = \int_{\Omega_1} \beta \nabla u \cdot \nabla v + \int_{\Omega_2} \beta \nabla u \cdot \nabla v + \int_{\Omega_3} \beta \nabla u \cdot \nabla v \tag{5.8}$$

Definition 5 1 1 $u \in H(a,c)$ is called a weak solution of equations 5 1-5 4, if it satisfies, for all $\psi \in H_0^1(\Omega)$,

$$\int_{\Omega_1} \beta \nabla u \quad \nabla\psi + \int_{\Omega_2} \beta \nabla u \quad \nabla\psi + \int_{\Omega_3} \beta \nabla u \quad \nabla\psi = \int_{\Omega} f\psi + \int_{\Gamma} b\psi \qquad (5\ 9)$$

Theorem 5 1 2 If $f \in L^2(\Omega)$, and a, b $\in H^1(\Omega)$, then there exists a unique weak solution of Equations 5 2-5 4

Proof See Theorem 2 1 in [15] □

5 2 Numerical Method

A cell K with corners k_1, k_2, k_3 belongs to one of three different sets

$$\begin{aligned}
\Lambda_1 &= \{\triangle_k \subset \Omega \quad k_1, k_2, k_3 \text{ are in the same domain among } \Omega_j,\ j = 1,2,3\}, \\
\Lambda_2 &= \{\triangle_k \subset \Omega \quad k_1, k_2, k_3 \text{ are in two different domains among } \Omega_j,\ j = 1,2,3\}, \\
\Lambda_3 &= \{\triangle_k \subset \Omega \quad k_1, k_2, k_3 \text{ are in three different domains among } \Omega_j,\ j = 1,2,3\}
\end{aligned}$$

If $K \in \Lambda_1$ or $K \in \Lambda_2$, it has the same definition as in Section 3 2, Chapter 3 If $K \in \Lambda_3$, Figure 5 2 shows the interfaces inside K

Theorem 5 2 1 For all $u^h \in H^{1,h}, U^h(u^h)$ can be constructed uniquely, provided T^h, ϕ, a and b are given

Proof See Theorem 3 2 1 in Chapter 3 □

Lemma 5 2 2 The coefficient matrix A generated by the method above is independent of $a_j(x,y)$ and $b_j(x,y)$, $j = 1,2,3$

Proof See Lemma 3 2 3 in Chapter 3 □

Theorem 5 2 3 The coefficient matrix $A = (a_{ij})_{n\times n}$ generated by the method above is positive definite if β_j, $j = 1,2,3$ are positive definite

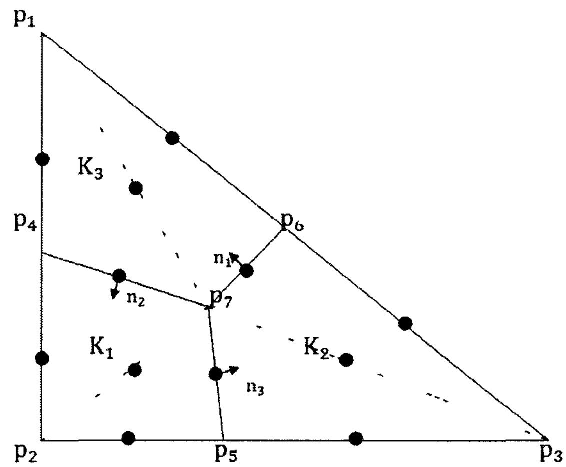

Figure 5 2 One triangle cell

Proof For any vector $c \in R^n$, $c^T A c > 0$ since

$$c^T A c = \sum_{i,j=1}^{n} a_{ij} c_i c_j = B\left[\sum_{i=1}^{n} c_i u^i, \sum_{i=1}^{n} c_i \psi^i\right], \tag{5 10}$$

where u^i are basis functions for the solution and ψ^i are the test functions For the i-th grid point, u^i and ψ^i both have non-zero support only on the six triangles which have a vertex on the i-th grid point u^i can be decomposed into $u^i = \sum_{j=1}^{6} u^i_j$, where each u^i_j has non-zero support only on the j-th triangle around the i-th grid point

Let m be the number of triangles on the whole domain $\Omega = \bigcup_{k=1}^{m} \triangle_k$ The summation of u^i over all the triangles can be rewritten

$$\sum_{i=1}^{n} c_i u^i = \sum_{i=1}^{n} \sum_{j=1}^{6} c_i u^i_j = \sum_{k=1}^{m} U_k, \tag{5 11}$$

where U_k is defined on $\triangle_k = \triangle_{k_1 k_2 k_3}$, and $U_k = c_{k_1} u_{k_1} + c_{k_2} u_{k_2} + c_{k_3} u_{k_3}$, k_1, k_2, k_3 are the three vertices of $\triangle_k$

Similarly, the summation of ψ^i over all the triangles can be rewritten

$$\sum_{i=1}^{n} c_i \psi^i = \sum_{i=1}^{n} \sum_{j=1}^{6} c_i \psi^i_j = \sum_{k=1}^{m} \Psi_k, \tag{5 12}$$

with

$$\Psi_k = c_{k_1}\psi_{k_1} + c_{k_2}\psi_{k_2} + c_{k_3}\psi_{k_3} \tag{5 13}$$

Consider the sets

$$\begin{aligned}
\Lambda_1 &= \{\triangle_k \subset \Omega \quad k_1, k_2, k_3 \text{ are in the same domain among } \Omega_j,\ j = 1,2,3\}, \\
\Lambda_2 &= \{\triangle_k \subset \Omega \quad k_1, k_2, k_3 \text{ are in two different domains among } \Omega_j,\ j = 1,2,3\}, \\
\Lambda_3 &= \{\triangle_k \subset \Omega \quad k_1, k_2, k_3 \text{ are in three different domains among } \Omega_j,\ j = 1,2,3\}
\end{aligned}$$

Then

$$\sum_{k=1}^{m} U_k = \sum_{\triangle_k \in \Lambda_1} U_k + \sum_{\triangle_k \in \Lambda_2} U_k + \sum_{\triangle_k \in \Lambda_3} U_k, \tag{5 14}$$

$$\sum_{k=1}^{m} \Psi_k = \sum_{\triangle_k \in \Lambda_1} \Psi_k + \sum_{\triangle_k \in \Lambda_2} \Psi_k + \sum_{\triangle_k \in \Lambda_3} \Psi_k \tag{5 15}$$

The difference between U_k and Ψ_k is, U_k satisfies the jump conditions on the interface and Ψ_k is a simple linear function on $\triangle_k$ So when $\triangle_k \in \Lambda_1$, there is no jump in $\triangle_k$ Thus

$$U_k(x,y) = \Psi_k(x,y),\ (x,y) \in \triangle_k,\ \triangle_k \in \Lambda_1$$

When $\triangle_k \in \Lambda_2$, the proof of Theorem 3 2 4 in Chapter 3 shows that by adjusting the jump conditions $a_j(x,y)$ and $b_j(x,y)$, it can be obtained that

$$U_k(x,y) = \Psi_k(x,y),\ (x,y) \in \triangle_k,\ \triangle_k \in \Lambda_2$$

Now let $\triangle_k \in \Lambda_3$ It has already been shown that $U_k(k_j) = \Psi_k(k_j),\ j = 1,2,3$ and it needs to be shown that

$$U_k(x,y) = \Psi_k(x,y),\ \forall (x,y) \in \triangle_k$$

By the method used for computation, it is assumed that three interfaces Γ_1, Γ_2, and Γ_3 intersect at the point p_0 inside $\triangle_k$, and each Γ_j intersects with one side of $\triangle_k$ at the point p_j for $j = 1, 2, 3$, (see Figure 5 3)

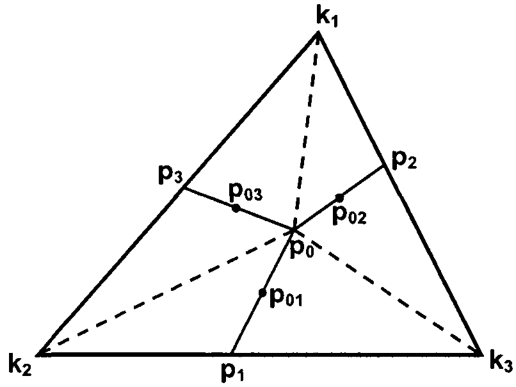

Figure 5 3 Interface triangle $\triangle_k$ belongs to Λ_3

Without loss of generality, it is assumed that $k_1 \in \Omega_1$, $k_2 \in \Omega_2$, and $k_3 \in \Omega_3$

First let

$$a_1(p_1) = 0,\ a_2(p_2) = 0,\ a_3(p_3) = 0,$$

and

$$a_1(p_0) = a_2(p_0) = a_3(p_0) = 0$$

Then $U_k(x, y)$ is piecewise linear on each sub-triangles $\triangle_{k_1p_0p_2}$, $\triangle_{k_1p_3p_0}$, $\triangle_{k_2p_0p_3}$, $\triangle_{k_2p_1p_0}$, $\triangle_{k_3p_0p_1}$, $\triangle_{k_3p_2p_0}$, and it can be determined by values at p_0, p_1, p_2, p_3 since $U_k(k_1)$, $U_k(k_2)$, $U_k(k_3)$ are given and fixed

First fix $U_k(p_0)$ and consider $\triangle_{k_2p_1p_0}$ and $\triangle_{k_3p_0p_1}$ It can be easily confirmed that when ranging $U_k(p_3)$ from $-\infty$ to ∞, $b_1(p_{01})$ also ranges from $-\infty$ to ∞, and vise versa Monotonicity implies $U_k(p_1)$ is uniquely determined by $b_1(p_{01})$ Similarly, $U_k(p_2)$ and $U_k(p_3)$ are uniquely determined by $b_2(p_{02})$ and $b_3(p_{03})$, respectively

Therefore, after applying jump conditions a_j and b_j for $j = 1, 2, 3$, the $U_k(x, y)$ is uniquely determined inside $\triangle_k$ corresponding to the value of $U_k(p_0)$

Then it is shown that $U_k(p_0)$ is unique after applying the conditions that $U_k(p_0)$, $U_k(p_1)$, $U_k(p_2)$ and $U_k(k_3)$ are in the same plane Suppose $U_k(x, y)$ and $V_k(x, y)$ are two piecewise linear functions which satisfy the same jump conditions a_j and b_j and value at p_0, p_1, p_2, and k_3 are in the same plane

If

$$U_k(p_0) = V_k(p_0),$$

then

$$U_k(x, y) = V_k(x, y), \ \forall (x, y) \in \triangle_k$$

If

$$U_k(p_0) \neq V_k(p_0),$$

and it is assumed

$$U_k(p_0) < V_k(p_0),$$

and since U_k and V_k both satisfy jump condition b_1 at p_{01}, it can be obtained that

$$U_k(p_1) > V_k(p_1)$$

Similarly, the result is

$$U_k(p_2) > V_k(p_2),$$

by applying jump condition b_2 at p_{02}

$U_k(p_0)$ and $V_k(p_0)$ can be also gotten by

$$\{U_k(p_1), \ U_k(p_1), \ U_k(k_3)\},$$

and

$$\{V_k(p_1),\ V_k(p_2),\ V_k(k_3)\},$$

respectively, since U_k and V_k are both linear functions on points p_0, p_1, p_2, and k_3

Since $U_k(k_3) = V_k(k_3)$, $U_k(p_1) > V_k(p_1)$, and $U_k(p_2) > V_k(p_2)$, it can be concluded that $U_k(p_0) > V_k(p_0)$ which contradicts the assumption that $U_k(p_0) < V_k(p_0)$

Therefore U_k is unique under these nine jump condition values $a_1(p_0)$, $a_1(p_1)$, $a_2(p_0)$, $a_2(p_2)$, $a_3(p_0)$, $a_3(p_3)$, $b_1(p_{01})$, $b_2(p_{02})$, and $b_3(p_{03})$ If those jump condition values are chosen under the function Ψ_k, then $U_k = \Psi_k$ in $\triangle_k$

Therefore

$$\sum_{\triangle_k \in \Lambda_3} U_k = \sum_{\triangle_k \in \Lambda_3} \Psi_k,$$

and the results are combined in Λ_j, $j = 1, 2, 3$ to get

$$\sum_{i=1}^{n} c_i u^i = \sum_{i=1}^{n} c_i \psi^i$$

It now follows from the positive definiteness of β that

$$c^T A c = B\left[\sum_{i=1}^{n} c_i u^i, \sum_{i=1}^{n} c_i \psi^i\right] > 0$$

Therefore, A is positive definite $\square$

From Remark 2 in Chapter 3, it is known that a positive definite matrix has positive determinant, and is therefore invertible The linear system $Ax = b$ can be solved efficiently

5 3 Numerical Experiments

In all examples of this section, the ϕ_j, β_j and u_j are given for $j = 1, 2, 3$ Hence f_j, a_j, b_j can be calculated on Ω g_j is obtained from the solutions as a proper Dirichlet boundary condition All errors in solutions are measured in the L^∞ norm in the whole domain Ω

Four numerical examples are presented in this chapter to demonstrate the effectiveness of this method

Example 12 This example has smooth interfaces which are two circles with the same center $\phi_j(x,y)$, $\beta_j(x,y)$ and $u_j(x,y)$ for $j = 1, 2, 3$, are given as

$$\phi_1(x,y) = x^2 + y^2 - 0\ 25^2, \tag{5 16}$$

$$\phi_2(x,y) = -(x^2 + y^2 - 0\ 5^2), \tag{5 17}$$

$$\phi_3(x,y) = x^2 + y^2 - 0\ 8^2, \tag{5 18}$$

$$\beta_1^+(x,y) = \begin{pmatrix} x^2+y^2+1 & x^2+y^2+2 \\ x^2+y^2+2 & x^2+y^2+5 \end{pmatrix}, \tag{5 19}$$

$$\beta_2^+(x,y) = \begin{pmatrix} x^2-y^2+3 & x^2-y^2+1 \\ x^2-y^2+1 & x^2-y^2+4 \end{pmatrix}, \tag{5 20}$$

$$\beta_3^+(x,y) = \begin{pmatrix} xy+2 & xy+1 \\ xy+1 & xy+3 \end{pmatrix}, \tag{5 21}$$

$$u_1(x,y) = x^2 + y^3 - 1, \tag{5 22}$$

$$u_2(x,y) = \cos(\pi x) + \cos(\pi y) + 2, \tag{5 23}$$

$$u_3(x,y) = 10x^2 + \sin(x+y) + 5 \tag{5 24}$$

The computed solution with the current method using a 40×40 grid is shown in Figure 5 4 Table 5 1 shows the error on different grids The numerical result shows close to second-order accuracy in the L^∞ norm for the solution

Example 13 Thıs example has two trıple junctıon poınts $\phi_j(x,y)$, $\beta_j(x,y)$ and $u_j(x,y)$ for $j = 1,2,3$, are gıven as

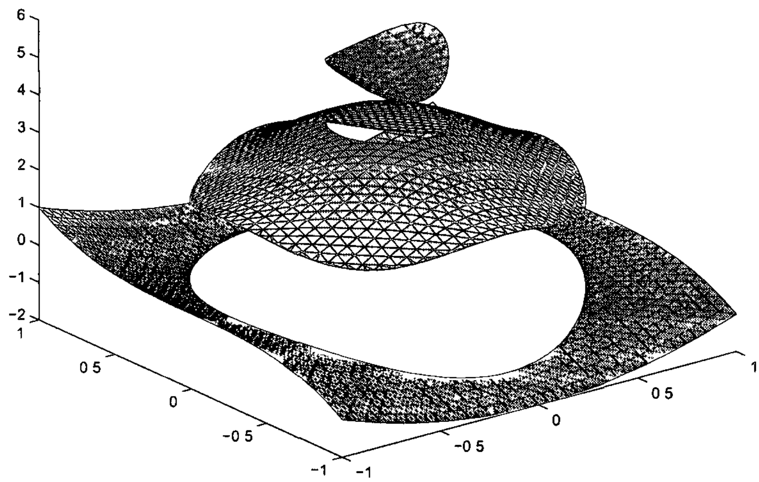

Fıgure 5 4 Interface wıth the shape of two cırcles

Table 5 1 Interface wıth the shape of two cırcles

$n_x \times n_y$	Error ın u	Order
20×20	9 7176e-003	
40×40	2 7138e-003	1 84
80×80	9 2766e-004	1 55
160×160	2 3779e-004	1 96

$$\phi_1(x,y) = -((x+0\ 17)^2 + y^2 - 0\ 317^2), \tag{5 25}$$

$$\phi_2(x,y) = (x-0\ 153)^2 + y^2 - 0\ 41^2, \tag{5 26}$$

$$\phi_3(x,y) = (x+0\ 17)^2 + y^2 - 0\ 317^2, \tag{5 27}$$

$$\beta_1^+(x,y) = \begin{pmatrix} x^2+y^2+1 & x^2+y^2+2 \\ x^2+y^2+2 & x^2+y^2+5 \end{pmatrix}, \quad (5\ 28)$$

$$\beta_2^+(x,y) = \begin{pmatrix} x^4+y^4+1 & x^4+y^4+2 \\ x^4+y^4+2 & x^4+y^4+5 \end{pmatrix}, \quad (5\ 29)$$

$$\beta_3^+(x,y) = \begin{pmatrix} x^2+y^4+1 & x^2+y^4+2 \\ x^2+y^4+2 & x^2+y^4+5 \end{pmatrix}, \quad (5\ 30)$$

$$u_1(x,y) = x + e^y + 1, \quad (5\ 31)$$

$$u_2(r,y) = \sin(2\pi x)\sin(2\pi y) + 6, \quad (5\ 32)$$

$$u_3(x,y) = x^2 + y^3 + \sin(x+y) \quad (5\ 33)$$

The computed solution with the current method using a 40×40 grid is shown in Figure 5 5 Table 5 2 shows the error on different grids The numerical result shows close to second-order accuracy in the L^∞ norm for the solution

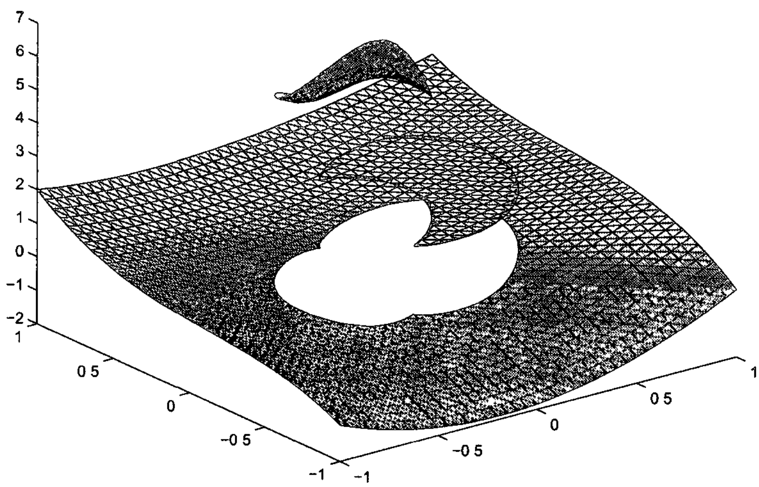

Figure 5 5 Interface with the shape of an eclipse

Example 14 This example is two circles touching each other $\phi_j(x,y)$, $\beta_j(x,y)$ and $u_j(x,y)$ for $j=1,2,3$, are given as

Table 5 2 Interface with the shape of an eclipse

$n_x \times n_y$	Error in U	Order
20×20	1 5022e-001	
40×40	5 4492e-002	1 46
80×80	1 6279e-002	1 74
160×160	4 3505e-003	1 90

$$\phi_1(x,y) = -((x+0\ 35)^2+y^2-0\ 35^2), \tag{5 34}$$

$$\phi_2(x,y) = (x-0\ 35)^2+y^2-0\ 35^2, \tag{5 35}$$

$$\phi_3(x,y) = x, \tag{5 36}$$

$$\beta_1^+(x,y) = \begin{pmatrix} x^2+y^2+1 & x^2+y^2+2 \\ x^2+y^2+2 & x^2+y^2+5 \end{pmatrix}, \tag{5 37}$$

$$\beta_2^+(x,y) = \begin{pmatrix} x^4+y^4+1 & x^4+y^4+2 \\ x^4+y^4+2 & x^4+y^4+5 \end{pmatrix}, \tag{5 38}$$

$$\beta_3^+(x,y) = \begin{pmatrix} x^2+y^4+1 & x^2+y^4+2 \\ x^2+y^4+2 & x^2+y^4+5 \end{pmatrix}, \tag{5 39}$$

$$u_1(x,y) = 5x+6y+1, \tag{5 40}$$

$$u_2(x,y) = -5x+6y+1, \tag{5 41}$$

$$u_3(x,y) = 2y^2+\sin(2\pi x)-2 \tag{5 42}$$

The computed solution with the current method using a 40×40 grid is shown in Figure 5 6 Table 5 3 shows the error on different grids The numerical result shows close to second-order accuracy in the L^∞ norm for the solution

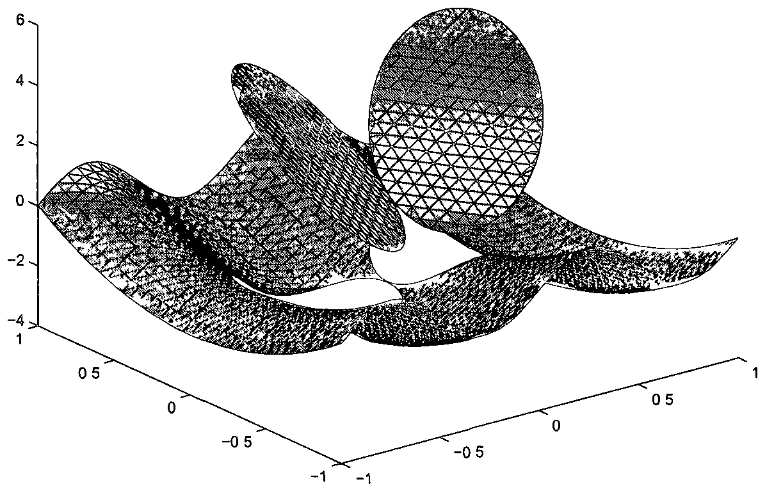

Figure 5 6 Two circles touching

Table 5 3 Two circles touching

$n_x \times n_y$	Error in U	Order
20×20	3 0337e-002	
40×40	9 5274e-003	1 67
80×80	2 6414e-003	1 85
160×160	7 7858e-004	1 76

Example 15 This example is a circle circumscribed on a star $\phi_j(x,y)$, $\beta_j(x,y)$ and $u_j(x,y)$ for $j = 1, 2, 3$, are given as

$$\phi_1(r,\theta) = -(\frac{R\sin(\theta_t/2)}{\sin(\theta_t/2 + \theta - \theta_r - 2\pi(i-1)/5)} - r$$

$$\theta_r + \pi(2i-2)/5 \le \theta < \theta_r + \pi(2i-1)/5, \tag{5 43}$$

$$\phi_1(r,\theta) = -(\frac{R\sin(\theta_t/2)}{\sin(\theta_t/2 - \theta + \theta_r - 2\pi(i-1)/5)} - r$$

$$\theta_r + \pi(2i-3)/5 \le \theta < \theta_r + \pi(2i-2)/5, \tag{5 44}$$

with $\theta_t = \pi/5,\ \theta_r = \pi/7,\ R = 6/7$ and $i = 1,2,3,4,5,$

$$\phi_2(x,y) = x^2 + y^2 - (6/7)^2, \tag{5 45}$$

$$\phi_3(x,y) = -(x^2 + y^2 - (6/7)^2), \tag{5 46}$$

$$\beta_1^+(r,y) = \begin{pmatrix} x^2+y^2+1 & x^2+y^2+2 \\ x^2+y^2+2 & x^2+y^2+5 \end{pmatrix}, \tag{5 47}$$

$$\beta_2^+(x,y) = \begin{pmatrix} x^2-y^2+3 & x^2-y^2+1 \\ x^2-y^2+1 & x^2-y^2+4 \end{pmatrix}, \tag{5 48}$$

$$\beta_3^+(x,y) = \begin{pmatrix} xy+2 & xy+1 \\ xy+1 & xy+3 \end{pmatrix}, \tag{5 49}$$

$$u_1(x,y) = 2y + 1 + 0\ 1\sin(2\pi(x^2+y)), \tag{5 50}$$

$$u_2(x,y) = 0, \tag{5 51}$$

$$u_3(x,y) = y^3 + e^x + 1 \tag{5 52}$$

The computed solution with the current method using a 40×40 grid is shown in Figure 5 7 Table 5 4 shows the error on different grids The numerical result shows close to second-order accuracy in the L^∞ norm for the solution

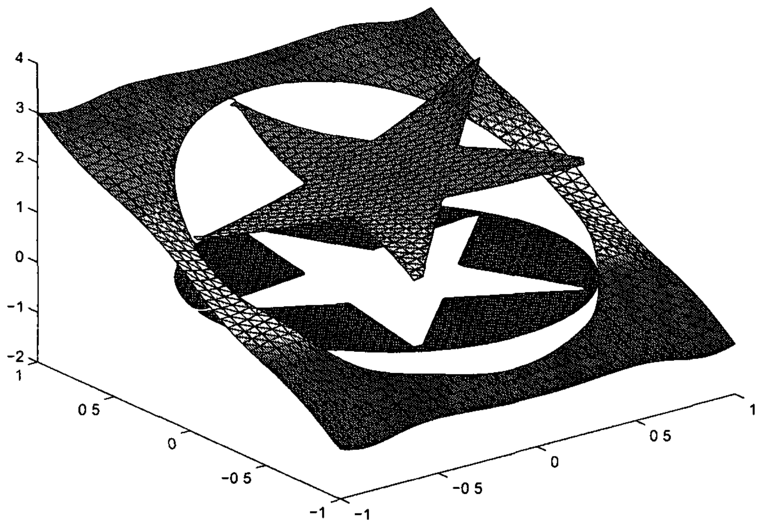

Figure 5 7 Interface with the shape of a star in a circle

Table 5 4 Interface with the shape of a star in a circle

$n_x \times n_y$	Error in U	Order
20×20	4 5391e-002	
40×40	1 7135e-002	1 41
80×80	5 2382e-003	1 71
160×160	1 3995e-003	1 90

CHAPTER 6

3-D ELLIPTIC PROBLEM WITH TWO DOMAINS

In this chapter, a three-dimensional model is developed to solve the elliptic interface problem with two domains The resulting linear system in three dimensions is also proved to be positive definite but not symmetric Four examples are given, numerical results show that the three-dimensional model is second-order accurate In all the examples, the interfaces contain sharp corners, which means that this method also works for the sharp interface problem

6 1 Equations and Weak Formulations

The variable coefficient elliptic interface problem is given by

$$-\nabla \cdot (\beta(x) \nabla u(x)) = f(x), \quad x \in \Omega \setminus \Gamma, \tag{6 1}$$

where $x = (x_1, \ldots, x_d)$ is the spatial variables $\beta(x)$ is a $d \times d$ matrix that is uniformly elliptic on each disjoint subdomain, Ω^- and Ω^+ $f(x)$ is in $L^2(\Omega)$

The jump conditions are prescribed as

$$\begin{cases} [u]_\Gamma(x) \equiv u^+(x) - u^-(x) = a(x), \\ [(\beta \nabla u) \cdot n]_\Gamma(x) \equiv n \cdot (\beta^+(x) \nabla u^+(x)) - n \cdot (\beta^-(x) \nabla u^-(x)) = b(x), \end{cases} \tag{6 2}$$

a and b are given functions along Γ, " $\pm$ " denote limits taken within $\Omega^\pm$

Function g is given on $\partial\Omega$, the boundary condition is prescribed as

$$u(x) = g(x), \quad x \in \partial\Omega \tag{6 3}$$

The setup of the problem is illustrated in Figure 6 1

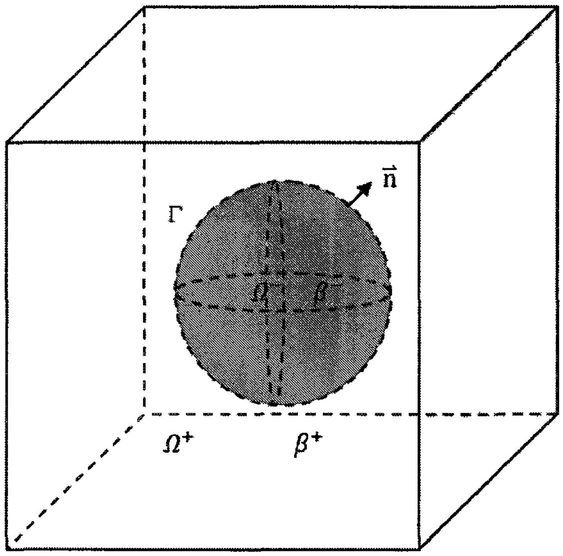

Figure 6 1 Setup of the problem

The weak formulation is generalized in [15, 16] for the elliptic equation with matrix coefficients The usual Sobolev space $H^1(\Omega)$ is used For $H_0^1(\Omega)$, an inner product is chosen as

$$B[u, v] = \int_{\Omega^+} \beta \nabla u \quad \nabla v + \int_{\Omega^-} \beta \nabla u \quad \nabla v \tag{6 4}$$

Definition 6 1 1 $u \in H(a, c)$ is called a weak solution of Equations 6 1-6 3, if u satisfies, for all $\psi \in H_0^1(\Omega)$,

$$\int_{\Omega^+} \beta \nabla u \quad \nabla \psi + \int_{\Omega^-} \beta \nabla u \quad \nabla \psi = \int_{\Omega} f\psi + \int_{\Gamma} b\psi \tag{6 5}$$

Theorem 6 1 2 If $f \in L^2(\Omega)$, a, b and $c \in H^1(\Omega)$, then there exists a unique weak solution of Equations 6 1-6 3 in $H(a, c)$

Proof See Theorem 2 1 in [15] □

6 2 Numerical Method

For simplicity, the setup is restricted to a cube cell domain $\Omega = (x_{min}, x_{max}) \times (y_{min}, y_{max}) \times (z_{min}, z_{max})$ in three-dimensional space, and β is a 3×3 matrix that is uniformly elliptic in each subdomain Given positive integers I, J and K, set $\Delta x = (x_{max} - x_{min})/I$, $\Delta y = (y_{max} - y_{min})/J$ and $\Delta z = (z_{max} - z_{min})/K$ A uniform Cartesian grid is defined as $(x_i, y_j, z_k) = (x_{min} + i\Delta x, y_{min} + j\Delta y, z_{min} + k\Delta z)$ for $i = 0, \quad , I$, $j = 0, \quad , J$ and $k = 0, \quad , K$ Each (x_i, y_j, z_k) is called a grid point $h = max(\Delta x, \Delta y, \Delta z) > 0$ is the grid size

Two grid functions sets will be used

$$H^{1,h} = \{\omega^h = (\omega_{i,j,k}) \quad 0 \le i \le I, 0 \le j \le J, 0 \le k \le K\},$$

and

$$H_0^{1,h} = \{\omega^h = (\omega_{i,j,k}) \in H^{1,h} \quad \omega_{i,j,k} = 0 \text{ if } i = 0, I \text{ or } j = 0, J \text{ or } k = 0, K\}$$

Every cube cell region $[x_i, x_{i+1}] \times [y_j, y_{j+1}] \times [z_k, z_{k+1}]$ is cut into six tetrahedron regions The tetrahedron regions are collected, and a uniform tetrahedralization $T^h \quad \bigcup_{L \in T^h} L$ is obtained, (See Figure 6 2 and Figure 6 3)

If $\phi(x_i, y_j, z_k) \le 0$, the grid point (x_i, y_j, z_k) is counted as in $\overline{\Omega^-}$, otherwise it is counted as in Ω^+

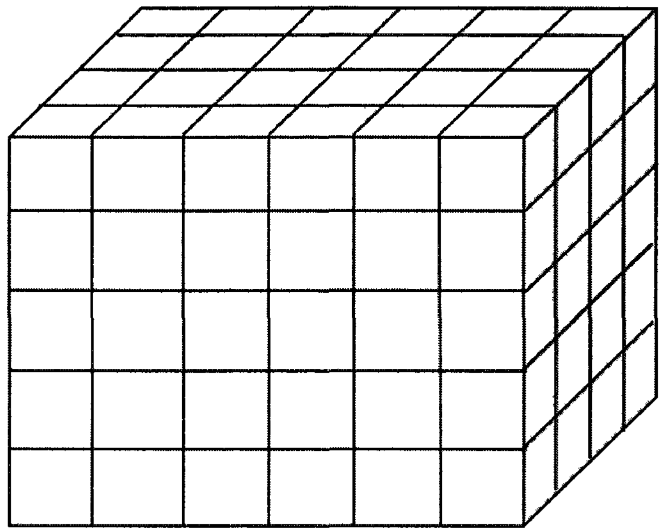

Figure 6 2 Cube cells of three-dimensional problems

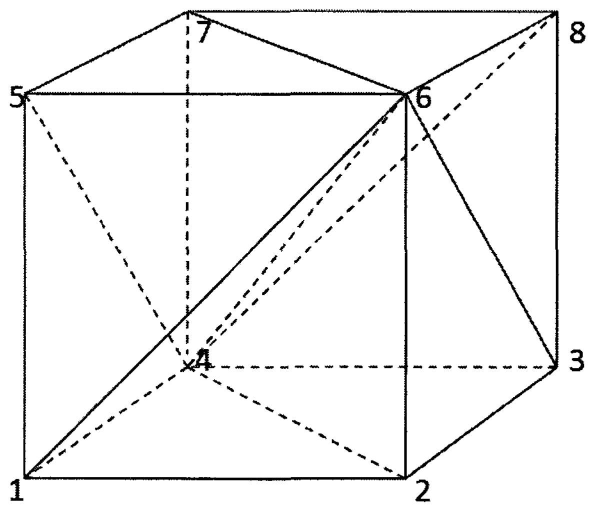

Figure 6 3 Tetrahedralization of three-dimensional problems

A cell $\blacktriangle_L$ with corners L_1, L_2, L_3, L_4 belongs to one of two different sets

$$\Lambda_1 = \{\blacktriangle_L \subset \Omega \quad L_1, L_2, L_3, L_4 \text{ are in the same domain among } \Omega^{\pm}\},$$

$$\Lambda_2 = \{\blacktriangle_L \subset \Omega \quad L_1, L_2, L_3, L_4 \text{ are in two different domains among } \Omega^{\pm}\}$$

If a cell belongs to Λ_1, it is a regular cell, otherwise it is an interface cell, written as $L = L^+ \bigcup L^-$ L^+ and L^- are separated by a plane segment, denoted by Γ_L^h There are two kinds of plane segments, see Figure 6 4 and Figure 6 5

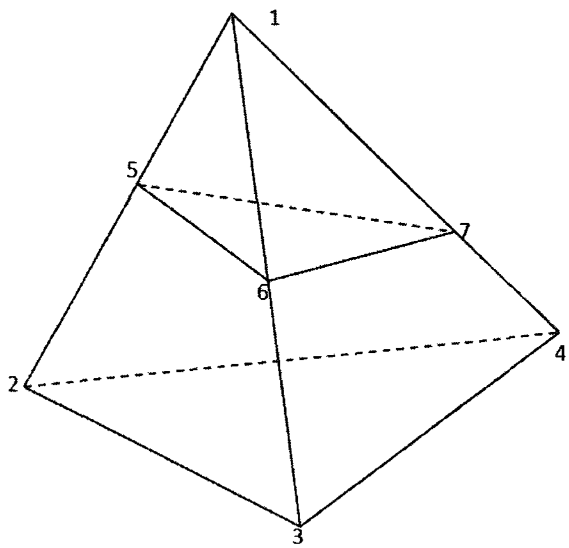

Figure 6 4 Case 1 The interface segment is a triangle

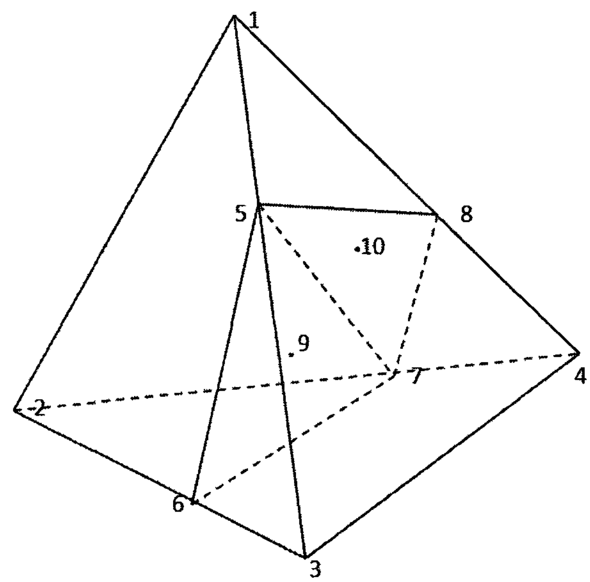

Figure 6 5 Case 2 The interface segment is a polygon

Since the solution bases and test function bases are different, the matrix A for the linear system generated by the current method is not symmetric in the presence of an interface. However, it can be proved that it is positive definite.

Theorem 6.2.1 If β is positive definite, then the $n \times n$ matrix A for the linear system generated by the current method is positive definite.

Proof. For any vector $c \in R^n$,

$$c^T A c = \sum_{i,j=1}^{n} a_{ij} c_i c_j = B\left[\sum_{i=1}^{n} c_i u^i, \sum_{i=1}^{n} c_i \psi^i\right],$$

where u^i and ψ^i are basis functions for the solution and the test function, respectively. Note that they have compact support and have nonzero values inside the 24 tetrahedra around the ith grid point. For ease of discussion, each of u^i and ψ^i is decomposed into 24 parts, so that each part has nonzero values only inside one tetrahedra. Now the summation over i is equivalent to a summation over all the tetrahedra, and there are four terms, $c_1u_1 + c_2u_2 + c_3u_3 + c_4u_4$, $c_1\psi_1 + c_2\psi_2 + c_3\psi_3 + c_4\psi_4$ for each tetrahedron, where $u_1, u_2, u_3, u_4, \psi_1, \psi_2, \psi_3, \psi_4$ equals 1 on one vertex of a tetrahedron and zero on three other vertices. The difference between u_i and ψ_i is, u_i depends on the location of the interface and ψ_i does not. $c_1u_1 + c_2u_2 + c_3u_3 + c_4u_4$ is a piecewise linear function satisfying the jump conditions and $c_1\psi_1 + c_2\psi_2 + c_3\psi_3 + c_4\psi_4$ is a linear function. At the four vertices, the two functions coincide. Now the jump conditions can be set as $a = 0$ and b can be set to have the value in the tetrahedron such that $c_1u_1 + c_2u_2 + c_3u_3 + c_4u_4 = c_1\psi_1 + c_2\psi_2 + c_3\psi_3 + c_4\psi_4$ everywhere. In other words, the jump in β is compensated by using b to make sure the gradients on both sides of the interface coincide. Since Lemma 3.2.2 and Lemma 3.2.3 in Chapter 3 imply the matrix A is independent of a, b, choosing the above a, b would not change the matrix A and would only change the constant term, i e , the right hand side of the linear system When the tetrahedra are summed all over, the result is

$$\sum_{i=1}^{n} c_i u^i = \sum_{i=1}^{n} c_i \psi^i$$

It now follows from the positive definiteness of β that

$$c^T A c = B\left[\sum_{i=1}^{n} c_i u^i, \sum_{i=1}^{n} c_i u^i\right] > 0$$

Therefore A is positive definite □

From Remark 2 in Chapter 3, it is known that a positive definite matrix has a positive determinant, and is therefore invertible The linear system $Ax = b$ can be solved efficiently

6 3 Numerical Experiments

Consider the problem

$$-\nabla \cdot (\beta \nabla u) + p \cdot \nabla u + qu = f, \text{ in } \Omega^{\pm}, \tag{6 6}$$

$$[u] = a, \text{ on } \Gamma, \tag{6 7}$$

$$[(\beta \nabla u) \cdot n] = b, \text{ on } \Gamma, \tag{6 8}$$

$$u = g, \text{ on } \partial\Omega, \tag{6 9}$$

on the domain $\Omega = (x_{min}, x_{max}) \times (y_{min}, y_{max}) \times (z_{min}, z_{max})$ Γ is an interface prescribed by the level-set function $\phi(x, y, z)$ $n = \frac{\nabla\phi}{|\nabla\phi|}$ is the unit normal vector of Γ pointing from Ω^- to Ω^+

In all examples of this section, given $\phi(x, y, z)$, $\beta^{\pm}(x, y, z)$ and

$$u = u^+(x, y, z), \text{ in } \Omega^+, \tag{6 10}$$

$$u = u^-(x, y, z), \text{ in } \Omega^-, \tag{6 11}$$

such that, on Ω

$$f = -\nabla \ (\beta \nabla u), \tag{6 12}$$

$$a = u^+ - u^-, \tag{6 13}$$

$$b = (\beta^+ \nabla u^+) \ n - (\beta^- \nabla u^-) \ n \tag{6 14}$$

g is obtained from the solutions as a proper Dirichlet boundary condition

All errors in solutions are measured in the L^∞ norm in the whole domain Ω

Example 16 The interface of this example is an intersection of a few balls $\beta^{\pm}$ and $u^{\pm}$ are

$$\beta^+(x, y, z) = \begin{pmatrix} 4\sin(x)^2 + 6 & \sin(y+x)z & yx \\ \sin(y+x)z & 2z^2 + \cos(x^2)^2 + 3 & 0\,5\sin(xy) \\ yx & 0\,5\sin(xy) & \cos(xy+z)^2 + 5 \end{pmatrix}, \tag{6 15}$$

$$\beta^-(x, y, z) = \begin{pmatrix} xz + \cos(x+y) + 3 & x & 0\,2\sin(y-x) \\ x & z^2 + 5 & yz \\ 0\,2\sin(y-x) & yz & \sin(z)^2 + 2 \end{pmatrix}, \tag{6 16}$$

$$u^+(x, y, z) = 10 - x^3 + 2y^2 - 2z + \sin(x+y+z) + \sin(x) + z, \tag{6 17}$$

$$u^-(x, y, z) = z^3 + y^2 - 2x \tag{6 18}$$

When the level-set function ϕ is given as

$$\phi(x, y, z) = \min((x - 0\,2)^2 + y^2 + z^2 - 0\,25, (x + 0\,2)^2 + y^2 + z^2 - 0\,25), \tag{6 19}$$

Figure 6 6 shows the computed error on the interface with the current method using 24 grid points in x, y and z directions, different colors denote different values of the error Table 6 1 shows the error on different grids

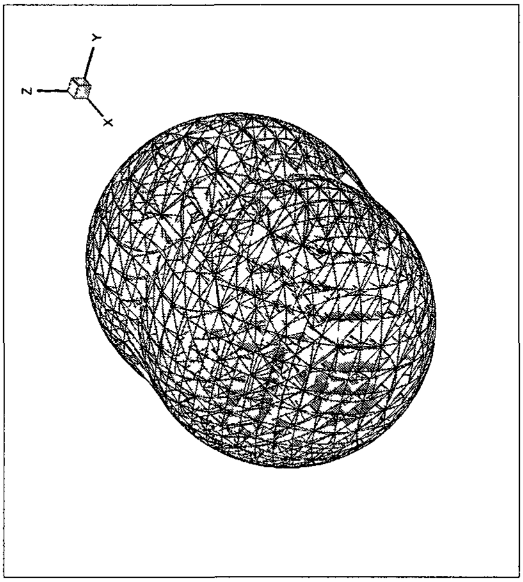

Figure 6 6 Intersection of two balls

Table 6 1 Intersection of two balls

$n_x \times n_y \times n_z$	Error in U	Order
$6 \times 6 \times 6$	0 02400	
$12 \times 12 \times 12$	0 00742	1 6944
$24 \times 24 \times 24$	0 00220	1 7557
$48 \times 48 \times 48$	0 00060	1 8746
$96 \times 96 \times 96$	0 00015	1 9909

When the level-set function ϕ is given as

$$
\begin{aligned}
\phi(x,y,z) &= \min(\min((x-0\ 4)^2+y^2+z^2-0\ 25, \\
&\qquad (x+0\ 3)^2+y^2+z^2)-0\ 25, x^2+(y+0\ 5)^2+z^2-0\ 25), \quad (6\ 20)
\end{aligned}
$$

Figure 6 7 shows the computed error on the interface with the current method using 24 grid points in x, y and z directions, different colors denote different values of the error Table 6 2 shows the error on different grids

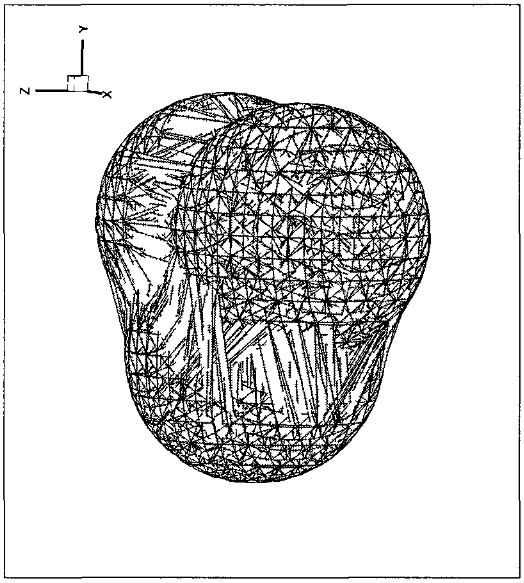

Figure 6 7 Intersection of three balls

When the level-set function ϕ is given as

$$
\begin{aligned}
\phi(r,y,z) &= \min(r^2+y^2+(z+0\ 5)^2-0\ 25, \min(\min((r-0\ 4)^2+y^2+z^2-0\ 25, \\
&\qquad (x+0\ 3)^2+y^2+z^2-0\ 25), x^2+(y+0\ 5)^2+z^2-0\ 25)), \qquad (6\ 21)
\end{aligned}
$$

Figure 6 8 shows the computed error on the interface with the current method using 24 grid points in x, y and z directions, different colors denote different values of the error Table 6 3 shows the error on different grids

Table 6 2 Intersection of three balls

$n_x \times n_y \times n_z$	Error in U	Order
$6 \times 6 \times 6$	0 04143	
$12 \times 12 \times 12$	0 01427	1 5374
$24 \times 24 \times 24$	0 00370	1 9479
$48 \times 48 \times 48$	0 00100	1 8938
$96 \times 96 \times 96$	0 00025	2 0011

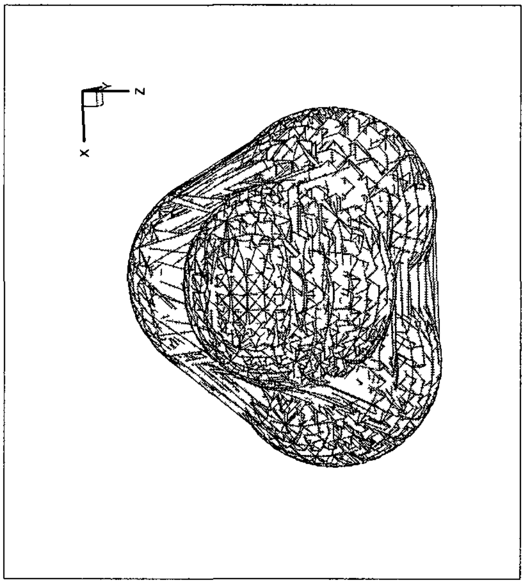

Figure 6 8 Intersection of four balls

Example 17 The interface of this example is an intersection of two balls ϕ, $u^{\pm}$ $\beta^{\pm}$ are

$$\phi(x,y,z) \quad = \quad \min((x-0\ 2)^2+y^2+z^2-0\ 25,(x+0\ 2)^2+y^2+z^2-0\ 25),$$

Table 6 3 Intersection of four balls

$n_x \times n_y \times n_z$	Error in U	Order
$6 \times 6 \times 6$	0 04193	
$12 \times 12 \times 12$	0 01426	1 5556
$24 \times 24 \times 24$	0 00370	1 9467
$48 \times 48 \times 48$	0 00100	1 8939
$96 \times 96 \times 96$	0 00025	2 0010

$$\beta^+(x,y,z) = \begin{pmatrix} 4x^2+6 & \sin(y+x) & yx \\ \sin(y+x) & 2z^2+3 & 0\,5\sin(x) \\ yx & 0\,5\sin(x) & \cos(xy+z)^2+5 \end{pmatrix}, \quad (6\ 22)$$

$$\beta^-(x,y,z) = \begin{pmatrix} \cos(x+y)^2+3 & z & 0\,2\sin(z-x) \\ z & z^2+5 & y \\ 0\,2\sin(z-x) & y & \sin(z)^2+2 \end{pmatrix}, \quad (6\ 23)$$

$$u^+(x,y,z) = 10-2x^3+3y^2+\sin(z-y), \quad (6\ 24)$$

$$u^-(x,y,z) = -6\sin(x)+3y+5z^3 \quad (6\ 25)$$

Figure 6 9 shows the computed error on the interface with the current method using 24 grid points in x, y and z directions, different colors denote different values of the error Table 6 4 shows the error on different grids

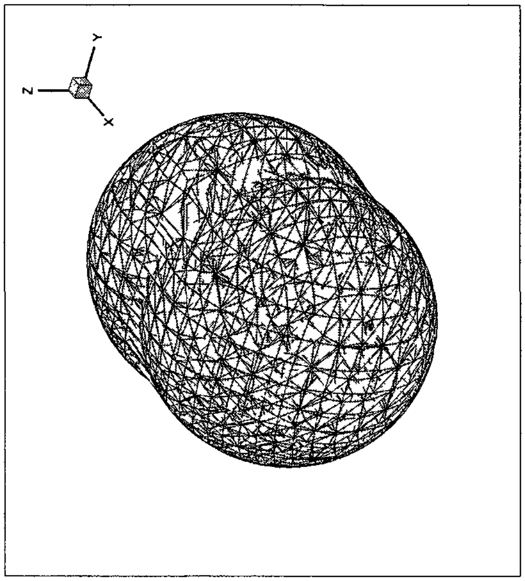

Figure 6 9 Example of three-dimensional problems Two balls 1

Table 6 4 Example of three-dimensional problems Two balls 1

$n_x \times n_y \times n_z$	Error in U	Order
$6 \times 6 \times 6$	0 05242	
$12 \times 12 \times 12$	0 01400	1 9043
$24 \times 24 \times 24$	0 00370	1 9204
$48 \times 48 \times 48$	0 00099	1 9036
$96 \times 96 \times 96$	0 00024	2 0141

Example 18 The interface of this example is also an intersection of two balls ϕ, $u^\pm$ and $\beta^\pm$ are

$$\phi(x, y, z) = \min((x - 0\ 2)^2 + y^2 + z^2 - 0\ 25, (x + 0\ 2)^2 + y^2 + z^2 - 0\ 25),$$

$$\beta^{+}(x,y,z) = \begin{pmatrix} 4x^2+6 & \sin(y+x) & yx \\ \sin(y+x) & 2z^2+3 & 0\ 5\sin(x) \\ yx & 0\ 5\sin(x) & \cos(xy+z)^2+5 \end{pmatrix}, \tag{6 26}$$

$$\beta^{-}(x,y,z) = \begin{pmatrix} \cos(x+y)^2+3 & z & 0\ 2\sin(z-x) \\ z & z^2+5 & y \\ 0\ 2\sin(z-x) & y & \sin(z)^2+2 \end{pmatrix}, \tag{6 27}$$

$$u^{+}(x,y,z) = 10\cos(x)\cos(y)\cos(z)+20, \tag{6 28}$$

$$u^{-}(x,y,z) = \exp(-(x^2+y^2+z^2)/20) \tag{6 29}$$

Figure 6 10 shows the computed error on the interface with the current method using 24 grid points in x, y and z directions, different colors denote different values of the error Table 6 5 shows the error on different grids

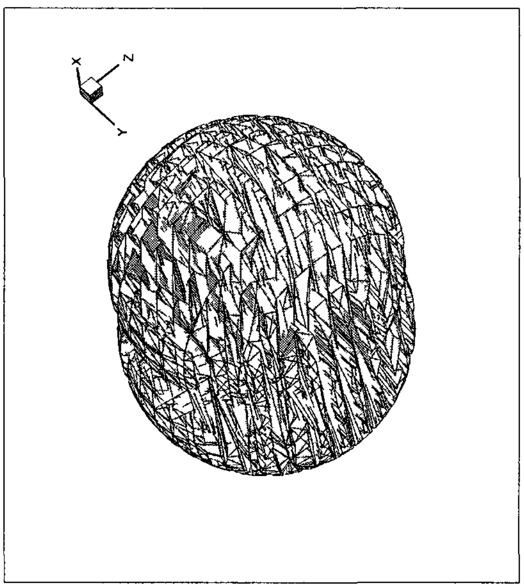

Figure 6 10 Example of three-dimensional problems Two balls 2

Table 6 5 Example of three-dimensional problems Two balls 2

$n_x \times n_y \times n_z$	Error in U	Order
$6 \times 6 \times 6$	0 10308	
$12 \times 12 \times 12$	0 02780	1 8909
$24 \times 24 \times 24$	0 00764	1 8628
$48 \times 48 \times 48$	0 00201	1 9254
$96 \times 96 \times 96$	0 00052	1 9441

Example 19 This example has a singular point on the interface ϕ, $u^{\pm}$ and $\beta^{\pm}$ are

$$\phi(x, y, z) = (x - 0\ 4)^2 + y^2 + z^2 - 0\ 16, \tag{6 30}$$

$$\beta^{+}(x, y, z) = \begin{pmatrix} 4x^2 + 6 & \sin(y + x) & yx \\ \sin(y + x) & 2z^2 + 3 & 0\ 5\sin(x) \\ yx & 0\ 5\sin(x) & \cos(xy + z)^2 + 5 \end{pmatrix}, \tag{6 31}$$

$$\beta^{-}(x, y, z) = \begin{pmatrix} \cos(x + y)^2 + 3 & z & 0\ 2\sin(z - x) \\ z & z^2 + 5 & y \\ 0\ 2\sin(z - x) & y & \sin(z)^2 + 2 \end{pmatrix}, \tag{6 32}$$

$$u^{+}(x, y, z) = (x^2 + y^2 + z^2)^{5/6}, \tag{6 33}$$

$$u^{-}(x, y, z) = \sin(x + y) \tag{6 34}$$

Figure 6 11 shows the computed error on the interface with the current method using 24 grid points in x, y and z directions, different colors denote different values of the error Table 6 6 shows the error on different grids

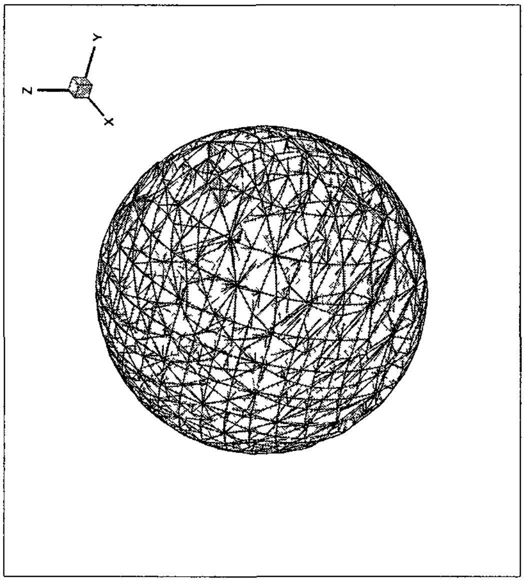

Figure 6 11 Singular point on the interface in three dimensions

Table 6 6 Singular point on the interface in three dimensions

$n_x \times n_y \times n_z$	Error in U	Order
$6 \times 6 \times 6$	0 02227	
$12 \times 12 \times 12$	0 00722	1 6262
$24 \times 24 \times 24$	0 00225	1 6816
$48 \times 48 \times 48$	0 00069	1 6951
$96 \times 96 \times 96$	0 00021	1 7208

CHAPTER 7

CONCLUSIONS AND FUTURE WORK

This dissertation extends the idea presented in [15] for solving matrix coefficient second-order elliptic equations for interface problems with two domains in two dimensions Parts of Chapter 3 have been published and can be found in [16]

This method is extended to solve second-order elasticity equations for interface problems with two domains in two dimensions, second-order elliptic equations for interface problems with three domains in two dimensions and second-order elliptic equations for interface problems with two domains in three dimensions This dissertation generalized the theorems in [15] and proofs are provided It is also proved that the matrix for the linear system generated by the current method is positive definite (but not symmetric) Through numerical experiments, this method achieved second-order accuracy in the L^∞ norm, and can handle the difficulties of sharp-edged interfaces and oscillatory solutions Compared with the previous work in [15], the order of accuracy for sharp-edged interfaces is improved from 0 8th to close to second order Compared with the result in [39], the more oscillatory the solution is, the more advantageous the current method is

The focus of the future work will be on the following topics

(1) Since the numerical results for two-dimensional/three-dimensional elliptic/elasticity

interface problems with two/three domains have been obtained, proofs of the convergence of this method for all the four topics will be the next step of research

(2) Elasticity interface problem with three domains in two dimensions

(3) Elliptic interface problem with three domains in three dimensions

(4) Elasticity interface problem with two domains in three dimensions

(5) Elasticity interface problem with three domains in three dimensions is a further extension of the above topics, it will be under consideration for future research

(6) Moving interface problems are more practical but yet more complicated Elliptic and elasticity problems with moving interface is another challenging research topic

(7) Some applications on solving the elliptic and elasticity interface problems, such as in biomathematics, fluid dynamics, etc

BIBLIOGRAPHY

[1] I Babuška The finıte element method for ellıptıc equatıons wıth dıscontınuous coefficıents *Computıng*, 5 207–213, 1970

[2] J Bedrossıan, J Von Brecht, S Zhu, E Sıfakıs, and J Teran A second order vırtual node method for poısson ınterface problems on ırregular domaıns *Journal of Computatıonal Physıcs*, 229 6405–6426, 2010

[3] J Bramble and J Kıng A finıte element method for ınterface problems ın domaıns wıth smooth boundarıes and ınterfaces *Advances ın Comput Math*, 6 109–138, 1996

[4] K Chan, K Zhang, X Lıao, J Zou, and G Schubert A three-dımensıonal spherıcal nonlınear ınterface dynamo *The Astrophysıcal Journal*, 596 663–679, 2003

[5] Z Chen and J Zou Fınıte element methods and theır convergence for ellıptıc and parabolıc ınterface problems *Numer Math*, 79 175–202, 1998

[6] Z M Chen and J Zou Fınıte element methods and theır convergence for ellıptıc and parabolıc ınterface problems *Numerısche Mathematık*, 79 175–202, 1998

[7] I L Chern and Y C Shu A couplıng ınterface method for ellıptıc ınterface problems *Journal of Computatıonal Physıcs*, 225 2138C2174, 2007

[8] P Colella and H Johansen A cartesian grid embedded boundary method for poisson's equation on irregular domains *Journal of Computational Physics*, 60 85–147, 1998

[9] L C Evans Partial differential equations *American Mathmetiacal Society*, 1998

[10] R Fedkiw, T Aslam, B Merriman, and S Osher A non-oscillatory eulerian approach to interfaces in multimaterial flows (the ghost fluid method) *Journal of Computational Physics*, 152 (2) 457–492, 1999

[11] Y Gong, B Li, and Z Li Immersed-interface finite-element methods for elliptic interface problems with non-homogeneous jump conditions *SIAM J Numer Anal*, 46 472–495, 2008

[12] Y Gong and Z Li Immersed interface finite element methods for elasticity interface problems with non-homogeneous jump conditions *Numerical Mathematics Theory, Methods and Applications*, in press

[13] P Grisvard Elliptic problems in nonsmooth domains c monographs and studies in mathematics *Pitman Advanced Publishing Program*, ISSN 0743-0329, 1985

[14] G Guyomarc'h, C Lee, and K Jeon A discontinuous galerkin method for elliptic interface problems with application to electroporation *Communications in Numerical Methods in Engineering*, 25 991–1008, 2009

[15] S M Hou and X D Liu A numerical method for solving variable coefficient elliptic equation with interfaces *Journal of Computational Physics*, 202 411–445, 2005

[16] S M Hou, W Wang, and L Q Wang Numerical method for solving matrix coefficient elliptic equation with sharp-edged interfaces *Journal of Computational Physics*, 229 7162–7179, 2010

[17] R J LeVeque and Z Li The immersed interface method for elliptic equations with discontinuous coefficients and singular sources *SIAM J Numer Anal*, 31 1019, 1994

[18] Z Li A fast iterative algorithm for elliptic interface problems *SIAM J Numer Anal*, 35 (1) 230–254, 1998

[19] Z Li The immersed interface method using a finite element formulation *Applied Numer Math*, 27 253–267, 1998

[20] Z Li, T Lin, and X Wu New cartesian grid methods for interface problems using the finite element formulation *Numerische Mathematik*, 9661-98 Preprint NCSU CRSC–TR99–12, 2003

[21] Z L Li and K Ito The immersed interface method Numerical solutions of pdes involving interfaces and irregular domains *SIAM, Philadelphia*, 2006

[22] X D Liu, R P Fedkiw, and M Kang A boundary condition capturing method for poisson's equation on irregular domains *Journal of Computational Physics*, 160 (1) 151–178, 2000

[23] X D Liu and T Sideris Convergence of the ghost fluid method for elliptic equations with interfaces *Math Comp*, 72 1731–1746, 2003

[24] P Macklin and J S Lowengrub A new ghost cell / level set method for moving boundary problems Application to tumor growth *Journal of Scientific Computing*, 35 266–299, 2008

[25] A Mayo The fast solution of poisson's and the biharmonic equations in irregular domains *SIAM J Numer Anal*, 21 (2) 285–299, 1984

[26] A Mayo Fast high order accurate solutions of laplace's equation on irregular domains *SIAM J Sci Stat Comput*, 6 (1) 144–157, 1985

[27] J Necas Introduction to the theory of nonlinear elliptic equations *TeubnerC-Texte zur Mathematik*, Band 52, ISSN 0138-502X, 1983

[28] M Oevermann and R Klein A cartesian grid finite volume method for elliptic equations with variable coefficients and embedded interfaces *Journal of Computational Physics*, 219 749–769, 2006

[29] M Oevermann, C Scharfenberg, and R Klein A sharp interface finite volume method for elliptic equations on cartesian grids *Journal of Computational Physics*, 228 5184–5206, 2009

[30] C Peskin Numerical analysis of blood flow in the heart *Journal of Computational Physics*, 25 220–252, 1977

[31] C Peskin and B Printz Improved volume conservation in the computation of flows with immersed elastic boundaries *Journal of Computational Physics*, 105 33–46, 1993

[32] M Sussman, P Smereka, and S Osher A level set approach for computing solutions to incompressible two-phase flow *Journal of Computational Physics*, 114 146–154, 1994

[33] Justin W L Wan and X D Liu A boundary condition capturing multigrid approach to irregular boundary problems *SIAM Journal on Scientific Computing*, 25 (6) 1982–2003, 2004

[34] K Xia, M Zhan, and G W Wei Mib method for elliptic equations with multimatherial interfaces *Journal of Computational Physics, in press*

[35] X Yang Immersed interface method for elasticity problems with interfaces *PhD thesis, North Carolina State University*, 2004

[36] X Yang, B Li, , and Z Li The immersed interface method for elasticity problems with interface *Dynamics of Continuous, Discrete and Impulsive Systems*, 10 783–808, 2003

[37] W -J Ying and C S Henriquez A kernel-free boundary integral method for elliptic boundary value problems *Journal of Computational Physics*, 227(2) 1046–1074, 2007

[38] S N Yu and G W Wei Three-dimensional matched interface and boundary (MIB) method for treating geometric singularities *Journal of Computational Physics*, 227 602–632, 2007

[39] S N Yu, Y C Zhou, and G W Wei Matched interface and boundary (MIB) method for elliptic problems with sharp-edged interfaces *Journal of Computational Physics*, 224 729–756, 2007

[40] Y C Zhou, S Zhao, M Feig, and G W Wei High order matched interface and boundary method for elliptic equations with discontinuous coefficients and singular sources *Journal of Computational Physics*, 213 1–30, 2006